Copyright

by

Alejandro Esteban Ortiz Pizzoglio

2017

The Thesis Committee for Alejandro Esteban Ortiz Pizzoglio
Certifies that this is the approved version of the following thesis:

Simulation of Stress Field Condition During Waller Creek Tunnel Construction with a 2D Finite Element Model

APPROVED BY
SUPERVISING COMMITTEE:

Supervisor:

Robert B. Gilbert, Supervisor

André Pacheco de Assis, Reader

Simulation of Stress Field Condition During Waller Creek Tunnel Construction with a 2D Finite Element Model

by

Alejandro Esteban Ortiz Pizzoglio

Thesis

Presented to the Faculty of the Graduate School of

The University of Texas at Austin

in Partial Fulfillment

of the Requirements

for the Degree of

Master of Science in Engineering

The University of Texas at Austin

August 2017

Dedication

To my grandfather, Italo Pizzoglio (†), and his memories that developed my curiosity for engineering.

To my family and friends.

Acknowledgements

First, I would like to express my deepest gratitude to my advisor, Dr. Robert Gilbert, for giving me the opportunity to work on this thesis and understanding my idea when I asked him I wanted to learn about tunneling. His patience, comments and advices encouraged me to enhance my skills and to increase even more my interest in tunneling projects.

I would also want to thank Dr. André Pacheco de Assis for accepting being the reader of my thesis and to Mr. Claude Berenguier for his numerous advices and for both, recommending me The University of Texas at Austin as a School for my grad studies in USA and moreover recommending me Dr. Assis as a reader. I would not like to forget to thank Mr. Roberto Gonzalez Izquierdo for always providing advices when I consulted him.

I would like to extend my gratitude to Fulbright Argentina, Gobierno de San Juan and UT Austin that gave me the possibility of pursuing a graduate course. Without their scholarship it wouldn't be possible.

A special mention is for my parents, Walter Ortiz and Rita Pizzoglio who always support and encouraged me to pursue my dreams. My brother, Patricio Ortiz Pizzoglio, and my sister, Silvina Ortiz Pizzoglio, also deserve my gratitude for always being there with advices. To Monica Taylor for being present in almost all my graduate program and for helped me to see a more positive perspective in difficult times. I also want to thank my friends from Argentina, specially to Andres Alonso, Juan Pablo Santiago and Nahuel Lahora that always have been present and supporting me.

I would like to thank to all those who I met in Austin. The group of Argentineans in Austin that always make me feel like home. I do not want to forget to the people I met

at UT, Ritika Sangroya Kundu, Ingrid Reyes Martinez, Wilfrido Martinez, Ricardo Dellamea, Gaston Quaglia, Leandro Montagna, Mario Glikman, Franco Di Biase, Amr Mosry, Hossein Roodi, Udit Dasgupta that provided me meaningful support and ideas during my grad course.

I would like to express my gratitude to Jesus Macedo, my Peruvian friend from Virginia Tech, with whom I started this experience abroad in 2015.

Finally, I would like to extend my appreciation to Alfredo Bocca, Joao Carlos Martins de Araujo and Juan Marcet for taking the time to write recommendation letters for me. Also I would like to thanks my colleagues from EICAM, Adriana Gomez, Maria Eugenia Ruiz, Susana Mengual, Alberto De Martini, Oscar Cordo, Pablo Girardi, Marcelo Bustos, etc for always helped me with advices.

Abstract

Simulation of Stress Field Condition During Waller Creek Tunnel Construction with a 2D Finite Element Model

Alejandro Esteban Ortiz Pizzoglio, M.S.E

The University of Texas at Austin, 2017

Supervisor: Robert Gilbert

Two-dimensional (2D) Finite Element Method (FEM) analyses are widely used as a tunnel design tool. These analyses are used to establish the initial support requirements, to estimate ground displacements and to design support systems to have adequate capacity and stiffness. Due to the complexities of ground characteristics, construction methods and the interactions between the ground and initial support lining systems, it is valuable to compare predictions from design analyses with field measurements.

The objective of this thesis is to compare FEM results with field measurements for stresses in an initial support lining system for a tunnel constructed in shale using the Sequential Excavation Method (SEM), the Waller Creek Tunnel in Austin, Texas. The major conclusion is that the predictions of liner stresses from FEM are greater than what was measured in the field, particularly for the thrust in the liner. While assuming that the ground is 20 times stiffer produces predictions closer to the measurements, the predictions are still greater, particularly for the thrust. One possible explanation for the discrepancy

between predications and measurements is that the stress cells did not have intimate contact with the liner.

Table of Contents

List of Tables

List of Figures

Chapter 1. Introduction

1.1 BACKGROUND

Two-dimensional (2D) Finite Element Method (FEM) analyses are widely used as a tunnel design tool. These analyses are used to establish the initial support requirements, to estimate ground displacements and to design support systems to have adequate capacity and stiffness. Due to the complexities of ground characteristics, construction methods and the interactions between the ground and initial support lining systems, it is valuable to compare predictions from design analyses with field measurements (e.g., Negro and de Queiroz 2000).

1.2 OBJECTIVES

The objective of this thesis is to compare FEM results with field measurements for stresses in an initial support lining system for a tunnel constructed in shale using the Sequential Excavation Method (SEM), the Waller Creek Tunnel in Austin, Texas.

1.3 ORGANIZATION

This thesis is organized in 7 chapters. Chapter 2 presents a background of the Waller Creek Tunnel project. Geographical information, tunnel cross section and alignment, and geology description are provided in this chapter. Furthermore, design considerations discussed.

Chapter 3 is an introduction to the FE analysis. Characteristics on how the ground is represented are provided.

In Chapter 4, the steps followed to simulate the Waller Creek Tunnel construction with the FE model are explained. At the end of this chapter, FEM outputs are provided.

Chapter 5 describes the stress cells used during construction to take radial stress and tangential stress readings and presents the measured data.

Chapter 6 provides a discussion between the output from the FEM and real field data.

Finally, Chapter 7, summarizes the results and provides guidance on actions to follow to try to improve the model output to better match the field data.

Chapter 2. Waller Creek Tunnel – General Information

Chapter 2 is intended to present an overview of the history of the project. Additionally, technical information about the design and rock characteristics are provided. This chapter intends to introduce the basic knowledge needed to understand the Waller Creek Tunnel Project.

2.1 INTRODUCTION

Downtown Austin has been suffering the consequences of flooding for many years. Since 1970, in order to reduce the risk associated with flooding events, the Waller Creek Tunnel project was a goal for the City of Austin. In 1999, a joint venture was contracted to develop the preliminary design, final design and construction management for the proposed Waller Creek Tunnel (WCT).

A view of the project site and the watershed considered for the design of Waller Creek Tunnel is presented in Figure 2.1.

The WCT project was estimated to cost over $100 million dollars. Five years of construction were expected, starting the construction in 2010 and completing it in 2014.

A 100-year flood event was used to the design of the diversion structure. The watershed considered for that purpose is a 1497 ha one. Here, the use of land includes a huge variety, from parks to family houses. A portion of the 176 ha of The University of Texas at Austin campus is part of the watershed. This watershed is one of the most developed watersheds of the tributaries of the Colorado River.

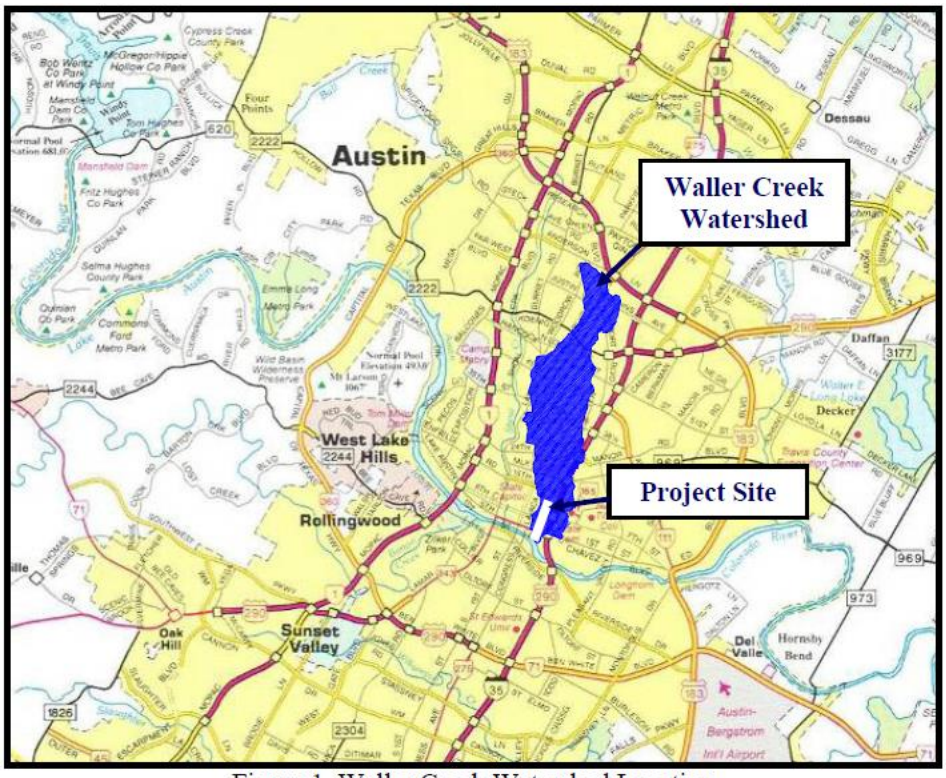

Figure 1. Waller Creek Watershed Location

Figure 2.1: Watershed Considered for the Waller Creek Tunnel (Waller Creek Tunnel Project, Austin, Texas. Reis and Espey, 2008)

2.2 LOCATION

Figure 2.2 presents a view of the project location. The project is located mainly below the Waller Creek from Waterloo Park to Lady Bird Lake. The main direction of the tunnel is North-South, parallel to I-35 and Red River Street.

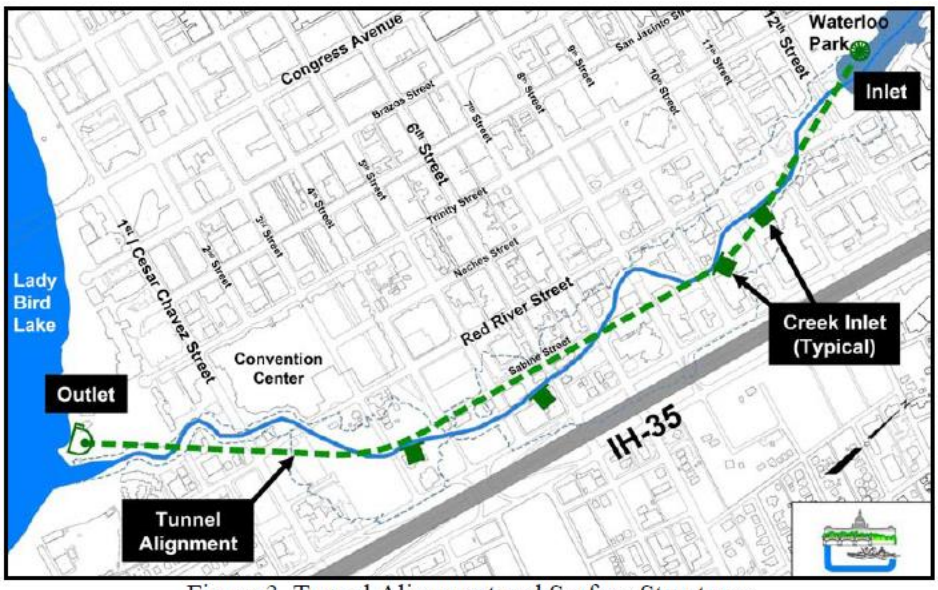

Figure 3. Tunnel Alignment and Surface Structures

Figure 2.2: Waller Creek Tunnel Alignment (Reis and Espey, 2008)

2.3 WALLER CREEK TUNNEL PROJECT

The tunnel project was intended to capture and divert floodwaters from the Waller Creek, includes an approximately 1600 meters length main tunnel with lateral connections to creek. Moreover, three reaches are part of the mainline tunnel, each of them identified for the different internal diameters. The diameters variy from 6.25m to 8.08m, Reach 1 has a 8.08, diameter, Reach 2 has a diameter of 6.86m and Reach 3 has 6.25m diameter. The different reaches are shown in Figure 3.1 Each reach is linked with the subsequent with a transition section between them. The cross-section shape of the tunnel is a horseshoe shape with flat bottom.

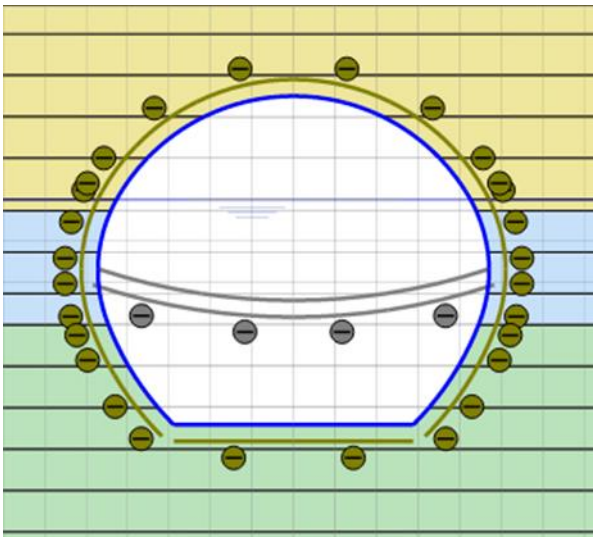

Figure 2.3: Horseshoe Shape with Flat Bottom

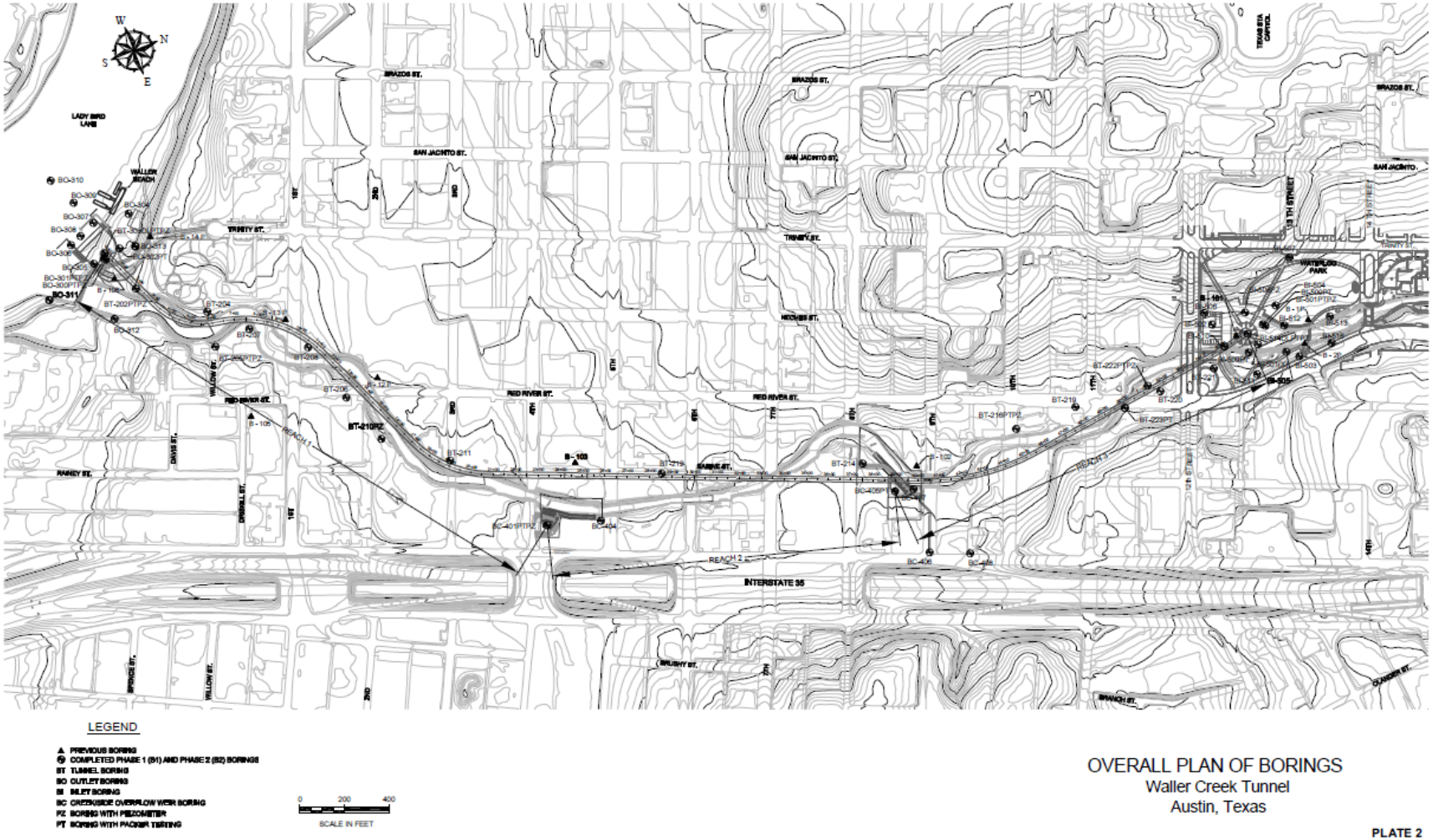

Figure 2.4: General Map of Waller Creek Tunnel (from Fugro)

2.4 GEOLOGY

A geological map of the Waller Creek Tunnel in Austin, Texas is presented in Figure 2.5. The site geology is entirely on sedimentary rocks, the tunnel was constructed through the Austin Group, Atco Formation Limestone (AFL) and Eagle Ford Shale (EFS). Four members of the EFS formation are present along the tunnel alignment, from top to bottom: South Bosque, Boulding Flags, Cloice and Peppershale.

Austin Group

Light gray to white chalk, marly limestone and limestone are included in this group. In general, the Austin Group (Limestone) was encountered without much degree of weathering.

Eagle Ford Shale

As mentioned above, South Bosque, Boulding Flags, Cloice and Peppershale are part of the EFS formation encountered from top to bottom, respectively, in the tunnel construction zone. The Peppershale is expected to be encountered only below the invert of the tunnel. On the other hand, the rest were expected to be founded as part of the cross section or in the full section.

Discontinuities

Faults with offset values less than 3m were found. Those fault characteristics had no significant impact in past tunnel constructions. Some fault gouge associated with faulting was encountered, without any significant influence during tunnel construction. Closed and tight joints and fractures were found in both, limestone and shale.

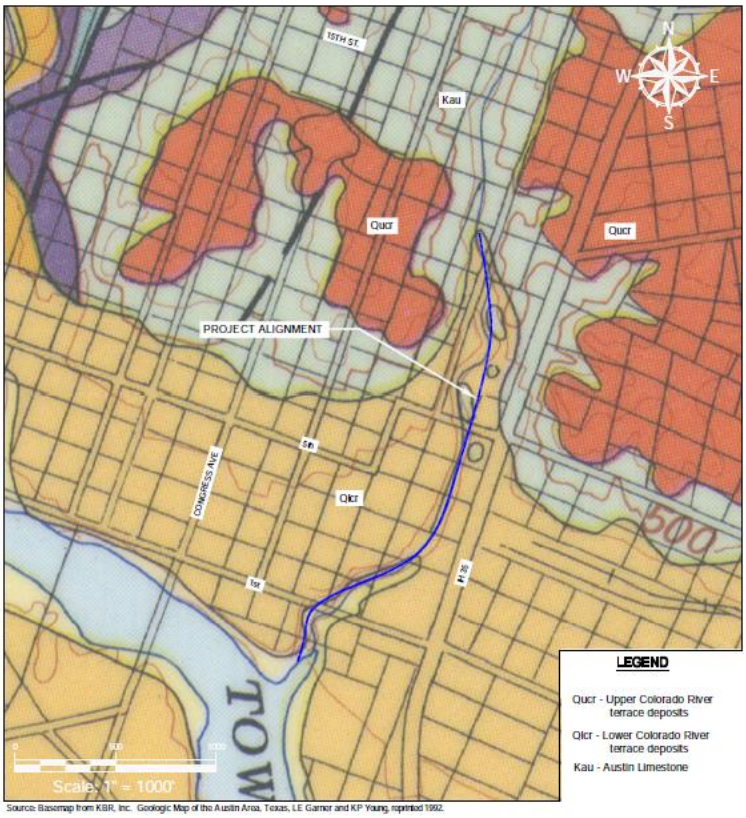

GEOLOGIC MAP
Waller Creek Tunnel
Austin, Texas

Figure 2.5: Geologic Map of Waller Creek Tunnel, Austin – Texas (From Fugro)

2.5 ROCK MASS CLASSIFICATION

Unconfined Compressive Strength, RQD, RMR and Q were used to estimate the rock quality of the rock for tunnel purposes. Table 2.1 presents the results from the Geotechnical Baseline Report or GBR (Jenny and KBR 2010). The rock mass classification presented in Table 2.1 shows the low quality the Eagle Ford Shale has in all the subgroups, with average RMR from 34 to 46. Moreover, when analyzing the rock quality based on the Q index proposed by Barton et al. (1974), it is possible to see how the rock quality only varies from "Very Poor" to "Poor" in all the cases.

Table 2.2 contains some characteristic indexes and strength of the Eagle Ford Shale formation such as Brazilian Tensile Strength, Point Load, Cerchar Abrasivity Index, Swell Pressure and Volume Change Potential.

Reach 3							
Geologic Unit			Unconfined Compressive Strength (MPa)	RQD	RMR	Q	Tunneling Rock Quality Based on Q Rating
Austin LS		Min.	0.17	7	21	0.4	Very Poor
		Ave.	13.61	84	54	20.8	Good
		Max.	31.52	100	67	25	Good
Eagle Ford Shale	South Bosque	Min.	1.32	45	16	0.2	Very Poor
		Ave.	5.54	87	34	09	Very Poor
		Max.	10.06	100	42	1	Poor
	Boulding Flags	Min.	6.66	45	23	0.2	Very Poor
		Ave.	8.34	81	42	1.6	Poor
		Max.	11.12	100	45	2	Poor
	Cloice	Min.	2.43	42	16	0.8	Very Poor
		Ave.	4.35	89	36	1.8	Poor
		Max.	9.65	100	42	2	Poor

Table 2.1: Unconfined Compressive Strength and Rock Mass Classification for Reach 3 from GBR (Jenny and KBR 2010).

	Eagle Ford Shale								
	South Bosque			Boulding Flags			Cloise		
Property	Min.	Ave.	Max.	Min.	Ave.	Max.	Min.	Ave.	Max.
Brazilian Tensile Strength (MPa)	0.14	1.60	2.74	0.46	0.86	1.25	0.46	0.85	1.25
Punch Penetration (N/m)	1225	1401	1576	700	1225	1576	700	1225	1576
Point Load (MPa)	0.15	0.35	0.59	0.06	0.26	0.43	0.22	0.64	1.07
Slake Durability (%)	84	91	94	81	89	96	91	94	96
Cerchar Abrasivity Index	0.3	0.4	0.6	0.3	0.4	0.4	0.2	0.3	0.4
Swell Pressure (kPa)	239.4	526.6	1053.3	119.70	NA	335.1	47.8	478.8	670.3
Volume Change Potential (%)	0.35	NA	3.0	0.24	NA	0.25	0.1	NA	5.5

Table 2.2: Eagle Ford Shale Properties from GBR (Jenny and KBR 2010).

2.6 SURFACE WATER AND GROUNDWATER

Minor water inflow was expected during tunnel construction. The main source of water inflow would be surface water infiltration from Lady Bird Lake and from the creek in the southeast reach, while some inflow from artesian conditions was expected in the northeast area of the project.

The flow of water in the tunnel was expected to be highly influenced by rainfall and the Waller Creek water level. Moreover, watershed surface infiltration was also expected to be an influent factor during floods.

Furthermore, low rock permeability was likely to be encountered as a result of the Packer tests results and piezometer observations. Table 2.3 presents the results of Packer tests.

Boring No.	Depth (m)	Geologic Unit	Permeability (k) (cm/sec)				
			34473 Pa	68947 Pa	103421 Pa	68947 Pa	34473 Pa
BI-500PT	5.64-30.5	Austin/EFS/ Buda	0	0	0	0	0
BT-202PTPZ	21.19-22.72	Austin/EFS	0	0	0	0	0
	22.72-24.24	EFS	0	3.3x10^-6	6.6x10^-6	0	0
	24.24-25.77	EFS	0	0	0	0	0
BT-222PTPZ	17.38-20.43	Austin/EFS	0	0	0	0	0
	20.43-23.48	EFS	0	0	0	0	0
	23.48-26.53	EFS	0	0	0	0	0
	26.53-29.58	EFS/Buda	0	0	0	0	0
BO-303DLPTPZ	17.23-20.28	EFS	0	0	2.21x10^-6	0	0
	20.28-23.33	EFS/Buda	0	0	4.42x10^-6	0	0
	23.33-26.38		0	0	2.21x10^-6	0	0

Table 2.3: Packer Tests Results on Eagle Ford Shale, from GBR (Jenny and KBR 2010).

2.7 EXCAVATION AND SUPPORT

The tunnel was designed to be constructed using roadheader equipment all along the different sections. Drill and Blast was considered as an alternative construction method.

Initial support was intended to be performed generally with rock dowels and shotcrete in limestone. In sections where the tunnel was entirely shale, lattice girders or steel ribs in conjunction with shotcrete were proposed to provide extra ground support when necessary. Seven support types where designed as different combinations of the above-mentioned elements and assigned specifically to each section (Jenny and KBR 2010). Type A, consist on steel ribs with shotcrete, Type B, lattice girders with shotcrete, Type C, rock dowels with

shotcrete. All those three corresponds to Reach 1. Reach 2, had assigned a support Type D, consisting on rock dowels with shotcrete. Finally, Reach 3, was assigned with three different types of support. Support Type E, consisting on rock dowels and shotcrete, Type F, lattice girders with shotcrete and Type G, the one used for this analysis, consisting on steel ribs with shotcrete.

Chapter 3. Waller Creek Tunnel – Finite Element Model

This chapter has the intention to describe the finite element model, input parameters and factors considered to simulate the in-situ conditions on the FEM of the Waller Creek Tunnel. Each assumption is explained and illustrated with figures.

Initially, most of the input was obtained from the data available on the Waller Creek Tunnel Geotechnical Baseline Report. Subsequently, data from construction was used to refine the input when appropriate.

3.1 INTRODUCTION

As explained in Chapter 2 and presented in Figure 3.1, the Waller Creek Tunnel was divided into 3 reaches. The reach of interest in this case is Reach 3, according to the diameter of the tunnel cross section, located north from 12th street (upstream). This reach is divided into 3 sections according to the geological conditions founded, as explained in the GBR.

Starting at Station 50+75 and extending all the way to the inlet facility at Station 55+00 is the analyzed reach 3b-2. This reach was selected due to the presence of Eagle Ford Shale in the whole tunnel cross section and were field data was obtained.

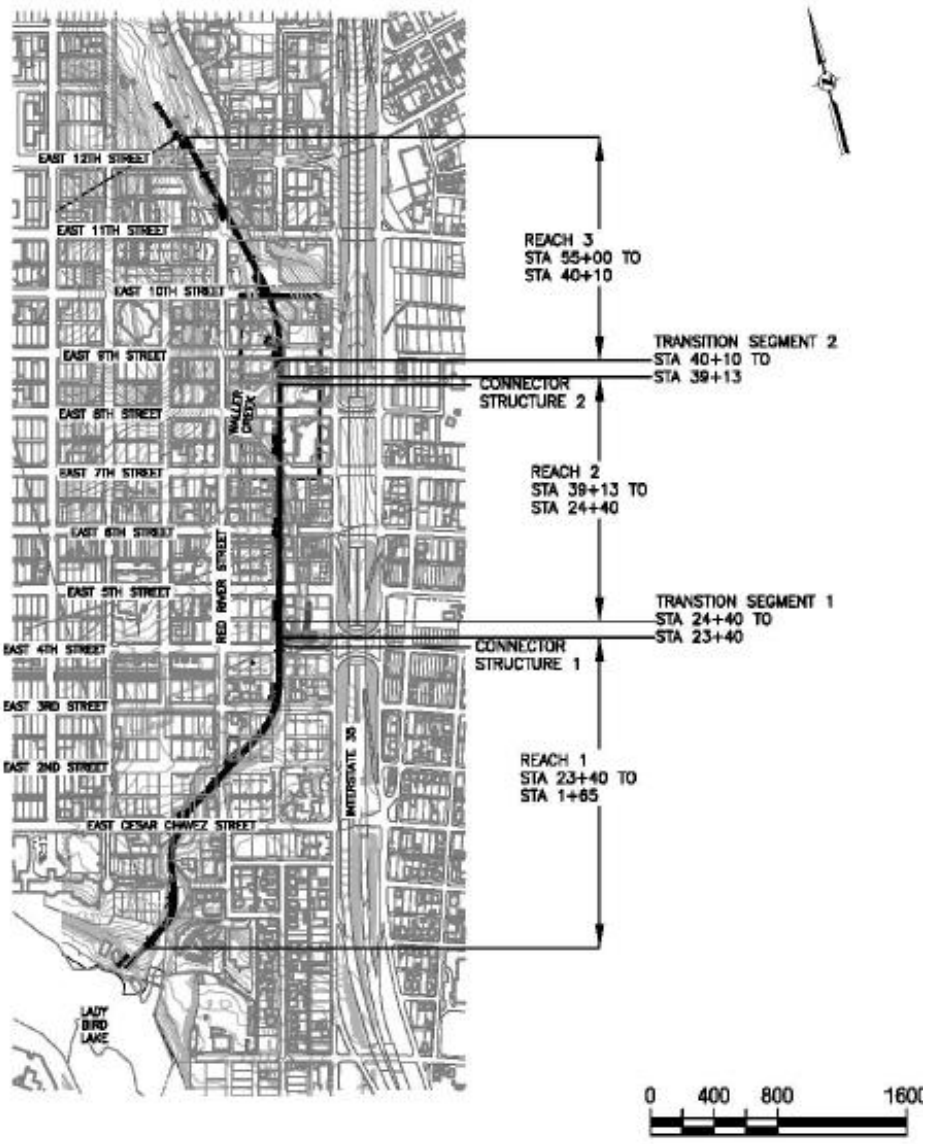

Figure 3.1: Waller Creek Tunnel Divided into 3 Reaches (From GBR)

A Finite Element Model of Reach 3b-2 from Waller Creek Tunnel was performed to simulate in-situ conditions during construction. The 2D FE analysis was selected since the length of a tunnel is considerably larger than the cross section, having an approximate plane strain condition. Special considerations were considered for the 3D arching effect during construction.

The plain strain scenario was modeled with the use of Plaxis 2D (Vermeer 1993), a finite element software developed for two-dimension deformation analyses.

3.2 MESH AND BOUNDARY CONDITIONS

Using the Geotechnical Baseline Report for the Waller Creek Tunnel Project, an underground soil profile was developed in Palxis 2D. For that purpose, a plane strain model was used with 15-Noded elements. 9409 soil elements were created in conjunction with 76056 nodes.

The selection for the model geometry prioritizes the reduction of the outer boundaries bias in the tunnel excavation results. For that purpose, distances from the center of the excavated tunnel to the outer boundaries were carefully selected. Height and width dimensions of 100 m were adopted for this model. The adopted width dimension fulfils Hoek's recommendation (Hoek 2000) of 3 times the radius from the center of the excavation to avoid the influence of the surrounding area during the simulation, leading to more accurate analysis.

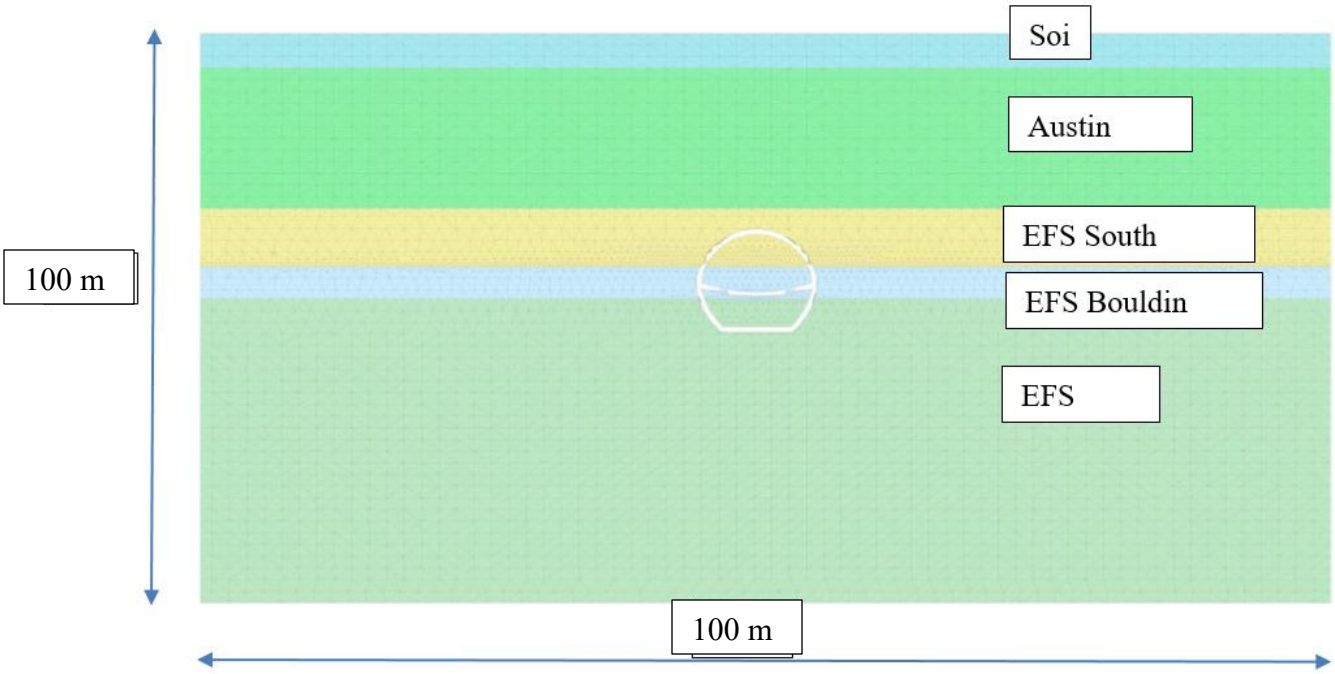

Figure 3.2: Waller Creek Tunnel Finite Element Model Mesh

3.3 STRATIFICATION

Three boreholes were created in the FE model to represent the stratification for this project. The representation of the different soil layers was carried out using an average layer thickness of 1m. The average thickness provides a dense mesh that produces more accurate results. For simplicity, horizontal layers were used in the model.

Five material types were represented. The upper layer is Top Layer Material. Below the soil of the top layer, Austin Chalk lays over the main body of Eagle Ford Shale. The Eagle Ford Shale is represented by 3 different subtypes, South Bosque Member, Bouldin Flags and Cloice Members from top to bottom respectively. Thickness of each ground group was adopted from the tunnel geological profile presented in Figure 3.4. The full tunnel excavation was performed in Eagle Ford Shale for the analyzed Reach 3b-2.

The 7.015m tunnel diameter has a minimum cover of 12.2m with a cover/diameter ratio of 1.7 as reported in the GBR.

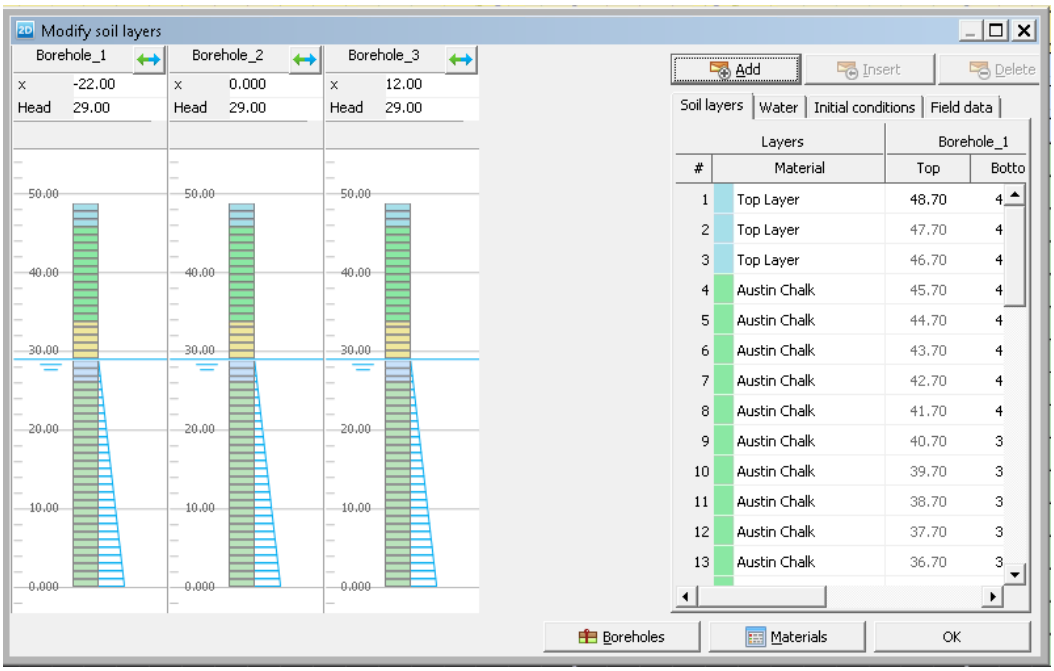

Figure 3.3: Stratification Proposed to Recreate the Underground Conditions

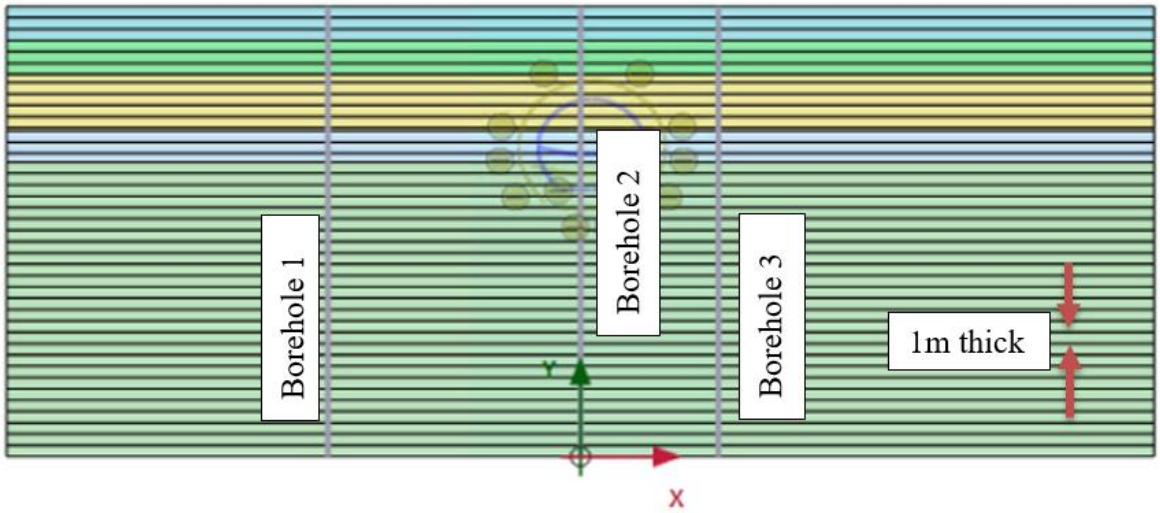

Figure 3.4: Stratification Proposed to Recreate the Underground Conditions

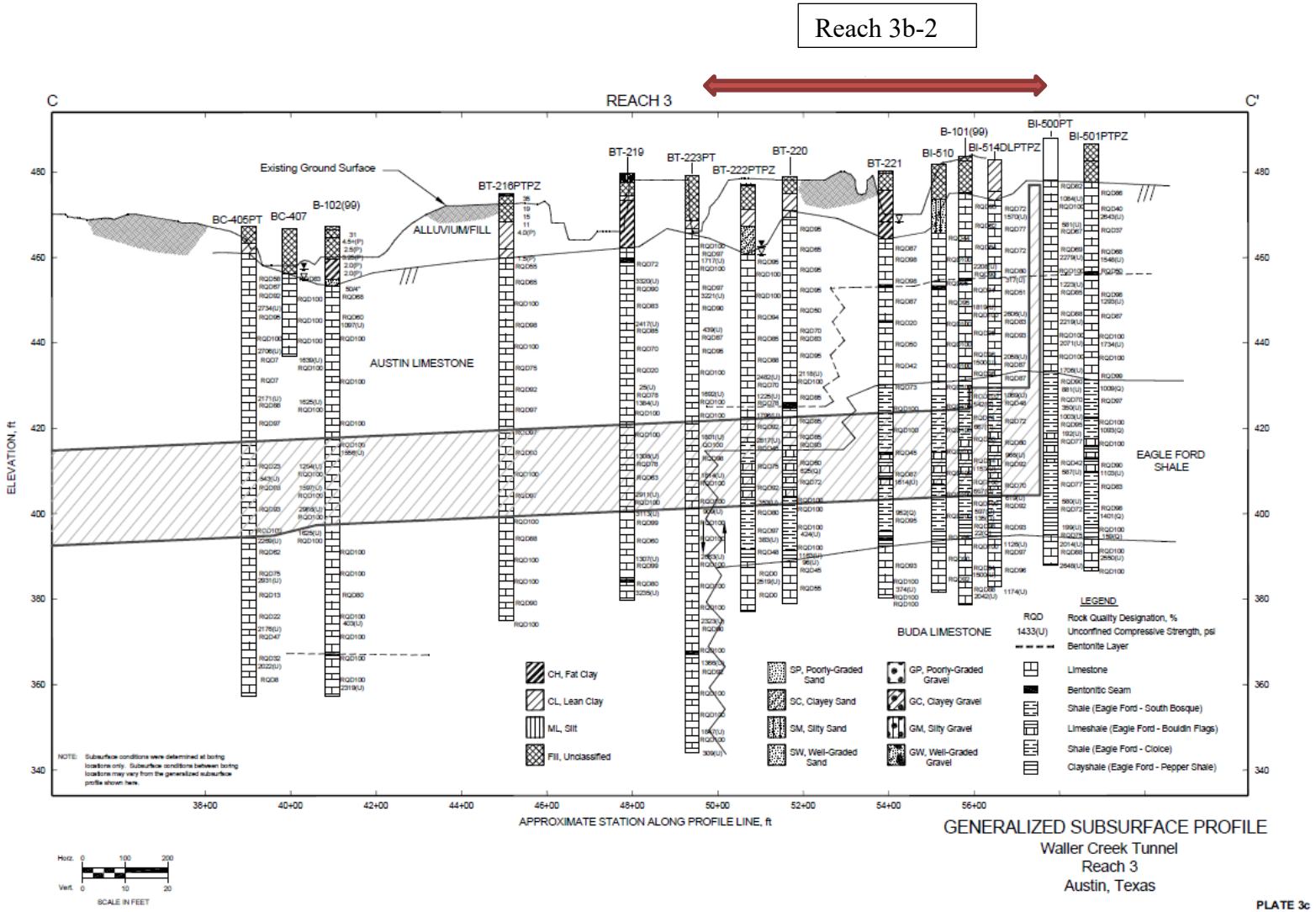

Figure 3.5: Geological Profile Analyzed to Create the FEM Ground Profile (Fugro)

3.4 GROUND PROPERTIES INPUT METHOD

The accuracy of the results is strongly related with the model selected to represent the mechanical behavior of the tunnel. As explained in Plaxis Manual, the easiest mode to represent a material is by simulating it with the Mohr-Coulomb linear-elastic model.

To represent the different ground materials, 3 different constitutive models were used. Soil of the top layer was modeled with the simplest characterization using the Mohr-Coulomb model. On the other hand, more complex models were used to model Austin Chalk and the different members of the Eagle Ford Shale.

As mentioned above, the linear elastic perfectly plastic model of Mohr-Coulomb was selected to represent the top soil layer. This constitutive model assumes a constant average stiffness for each layer. This constitutive model is recommended for first estimate of deformations.

For the Austin Chalk, an advanced constitutive model, the Hardening Soil Model, was selected. This model is an "elastoplastic type of hyperbolic model" as explained in Plaxis Material Models Manual.

A similar advanced constitutive model was adopted to be used by the all the types of Eagle Ford Shale, the Hardening Soil Model with Small-Strain Stiffness (HS Small). In this model, small to large strain reactions are simulated due to the incorporation of a strain dependent moduli.

3.5 DRAINAGE CONDITIONS

Pore pressure has a significant impact in the response on the FEM when using Plaxis since the model is analyzed in terms of effective stress response by the software. Short-term and long-term response are represented in Plaxis by the definition of the drainage type when simulating a simplified analysis. The HS Small constitutive model has 3 possible drainage types, Drained, Undrained (A) and Undrained (B).

Long-term conditions are represented by the Drained behavior. In this case, no pore water pressures are developed. This behavior is recommended for dry soils as well as high permeability soils, as explained by Plaxis in “Material and Material Database”.

When modeling short-term behavior or low permeability, undrained behavior is used to represent those situations. Modeling undrained behavior involves more difficulties. In this case, excess pore pressure is developed because of the lack of water movement.

Undrained (A) and Undrained (B) are the 2 drained types to represent these conditions. Each of them requires different drainage conditions in the input strength and stiffness parameters as explained by Helwa et.al. 2016.

In the case of Undrained (A), the undrained behavior is modeled by the use of effective parameters for both, stiffness and strength. On the other hand, undrained behavior can be modeled as Undrained (B) using undrained strength parameters and effective stress stiffness parameters.

The drainage condition of the analysis is independent of the input method used for the soil properties.

For this analysis, the short-term condition analysis was simulated by the use of drained conditions for the top soil layer and undrained (B) with no water pressure for the Eagle Ford Shale and the Austin Chalk.

3.6 GENERAL PROPERTIES

Both, saturated and unsaturated unit weight are defined for each layer.

When using dry unit weight, it is recommended not to use a value corresponding to completely dry unit weight in order to have a more accurate representation of the general properties of the soil since totally dry soil conditions are never found in the field.

First, unit weight estimations were done using an average specific gravity. Those results were later refined with some available data.

Table 3.1 presents a summary of the unit weight used in the FEM, while Figure 3.6 shows the input window in the software.

Name	γunsat	γsat
	kN/m3	kN/m3
Soil	19.64	19.64
Austin Chalk	23.88	25.55
EFS – South Bosque	19.64	21.32
EFS -Other	19.32	20.89

Table 3.1: Summary of the General Properties Used

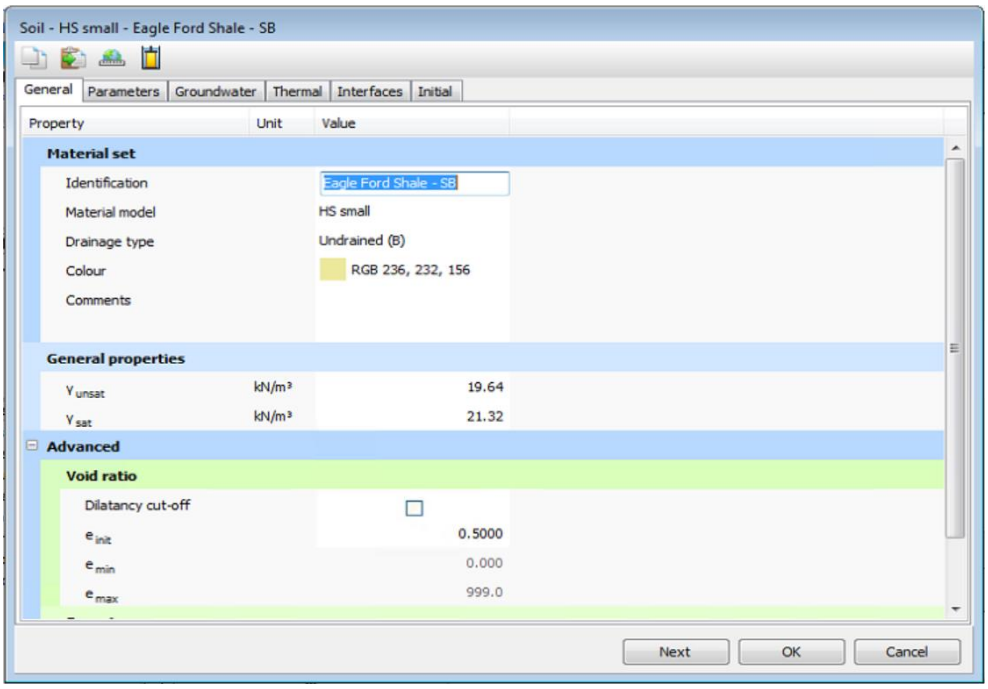

Figure 3.6: General Properties Input Window for Eagle Ford Shale – South Bosque

3.7 PARAMETERS

Strength and stiffness parameters are adopted to represent the ground characteristics in each case. The type of parameters as well as the number of parameters required are related with the constitutive model used. The input parameters were established based on the GBR (Jenny and KBR 2010) and the design calculations (Lachel 2012).

3.8 INTERFACE INTERACTION

Special attention is required when analyzing the soil structure interface area between the ground and the lining. There, the soil is still governed by the parameters selected for the surrounding soil. For the constitutive model selected to represent the behavior of the Eagle Ford Shale, HS Small, this interface is characterized by a strength reduction factor, Rinter. This factor is the main factor to simulate the real condition of the soil-structure interaction.

There are 3 main options offered by the software to represent the interface strength according to its characteristics, Rigid, Manual and Manual with Residual Strength.

Rigid: in the case there is no reduction in strength in the interface zone, the rigid option is the one that best represents this scenario. In this case, the factor Rinter is equal to 1.0.

Manual: Intended to allow the designer to better represent the weaker and more flexible characteristics of the interface in comparison to the surrounding soil. In this case, Rinter is less than one.

Manual with residual strength: With this option, the user allows the interface to soften down once the Rinter is reached until a defined Rinter residual value.

For this analysis, the strength reduction was set up as manual, using the values of Rinter of 0.8 for the top soil layer and 0.3 for the rest of the layers (Lachel 2012), as shown in Figure 3.7.

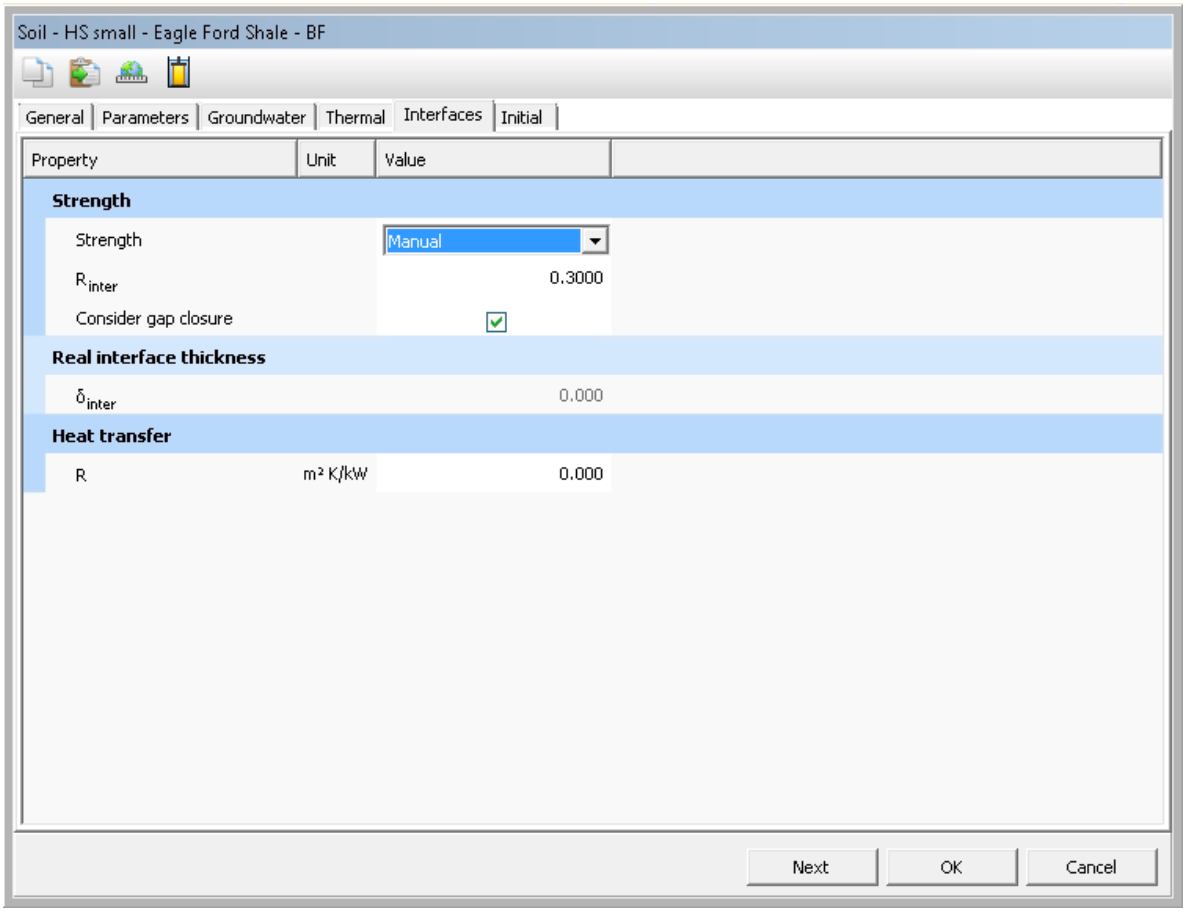

Figure 3.7: Interface Strength Characterized with the used of the Strength Reduction Parameter of 0.3 for Eagle Ford Shale.

3.9 INITIAL CONDITIONS

The initial stress conditions are defined in Plaxis using K0 procedure.

The definition of K0 can be done manually or automatically in the "Initial" tab-sheet as shown in Figure 3.8. The horizontal stress ratio is defined in terms of effective stresses.

In the case of advance constitutive models, such as the HS Small, K0 is defined by default as $K0^{NC}$.

The possibility of defining two different K0 parameters is offered by the FE software, counting for one horizontal stress ratio in the "x" direction and the other in the "z" direction, axis direction is presented in Figure 3.3. It is also possible to assign the same value of

horizontal stress ratio for both directions by selecting the corresponding checkbox showed in Figure 3.7.

$$k_{0,x} = \sigma'_{xx}/\sigma'_{yy}$$

$$k_{0,z} = \sigma'_{zz}/\sigma'_{yy}$$

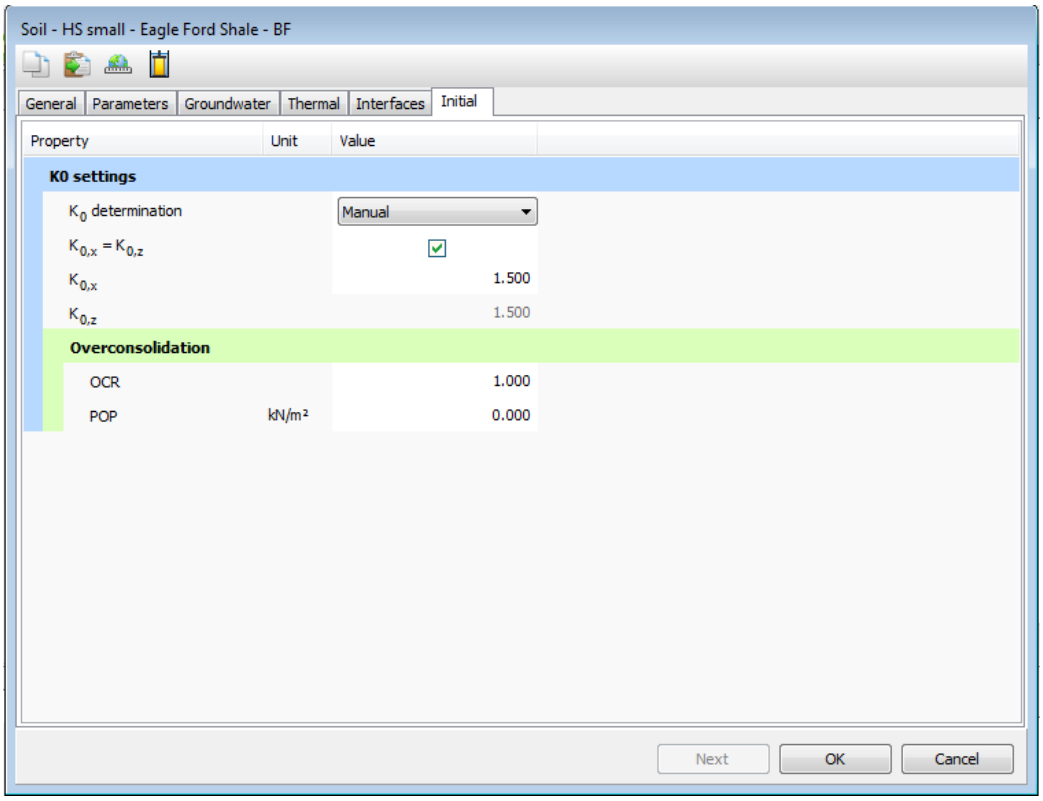

Figure 3.8: Initial Stress Conditions Using K0 Procedure.

For the analyzed Finite Element Model, the horizontal stress ratios used were, 1 for the top layer, 1.5 for the 3 different groups of Eagle Ford Shale, and 2.1 for the Austin Chalk (Lachel 2012). Those horizontal stress ratios were adopted from regional research measurement data.

3.10 Lining Properties

A common configuration of tunnel support is created by the use of shotcrete in conjunction with steel beams, as is the case of tunnel support Type G recommended in the

Waller Creek Tunnel GBR. Support Type G is composed by 15 cm thickness of shotcrete with W8x15 steel ribs (Table 3.2). During construction, steel ribs were placed at a spacing of 1.22 m. Poly Fiber Reinforced Shotcrete (PFRS) was used instead of ordinary Shotcrete; the influence of fibers is considered when calculating the PFRS Young's Modulus based on the Rule of Mixture (Voigt 1887):

Diameter of the fibers = 0.836mm (Equivalent Hydraulic Diameter)

Length of each poly fiber = 54mm

Fiber Dose = 5.94kg/m3

Minimum Fibers per kg = 37000/kg

Elastic Modulus of Poly Fibers = 9997 MPa

Elastic Modulus of Concrete = 27789 MPa

			Web	Flange		Elastic Properties					
	Area	Depth	Thickness	Width	Thickness	Axis X-X			Axis Y-Y		
	A	d	tw	bf	tf	Ix	Sx	rx	Iy	Sy	ry
Designation	in2	in	in	in	in	in4	in3	in	in4	in3	in
W8x15	4.4	8.11	0.245	4.015	0.315	48	11.8	3.29	3.41	1.7	0.88

Table 3.2: W8x15 Steel Beam Properties

Plate elements are the simplified model provided by FE software to model shotcrete when used as a liner. Two parameters are required to characterize the plate elements, normal stiffness (EA) and flexural rigidity (EI). As explained in "Analisis y Diseno Estructural de los Sistemas de Sostenimiento", Chapter 9 and according to Panet (1995), when a lining system composed by more than one element is analyzed, it is assumed that both elements, for example shotcrete and steel ribs in this case, are placed simultaneously during construction. As a consequence, it is possible to represent the mentioned system in a FEM by a unique plate element with a rigidity equivalent to both rigidities. The mechanical properties used for the finite element model are presented in Figure 3.9.

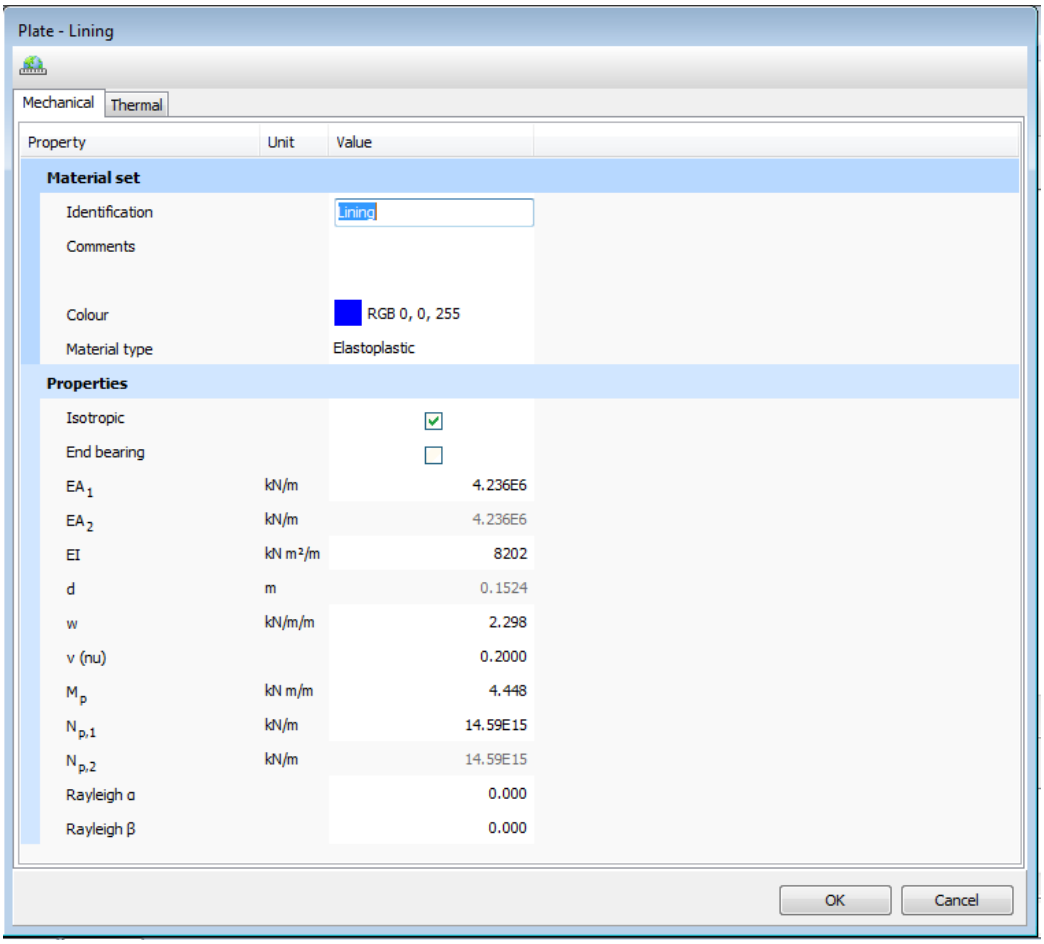

Figure 3.9: Lining Mechanical Properties

Chapter 4. FEM Construction Sequence and Results

Chapter 3 presented at the considerations and input data used to create the final element model. In this chapter, a description is provided of how the construction sequence was simulated in the FEM to represent possible the field conditions. At the end of the chapter, plots with the calculated displacements, thrust, shear and bending moments are presented. Moreover, a chart with specific results obtained from the crown and the spring-line are presented to correspond to the locations of field measurements.

4.1 CONSTRUCTION SEQUENCE

The construction sequence was simulated using an initial phase plus 4 sequential phases of excavation. The first phase is excavation of the top heading of the tunnel 2.44m in front of the existing initial support. The ground supports itself in the section via arching. The next step is the installation of the shotcrete and steel ribs in this opened top heading (i.e., two sets of ribs). First a 5-cm thick flash is applied. Then, the 2 new ribs were installed and blocked to the ground using hardwood. Last, a 10-cm thick layer of shotcrete was applied. The field instrumentation was placed at this step. The phase is continued excavation of the top heading beyond this section loading the initial support in this section. The third phase of excavation of the bottom bench of the tunnel 2.44m in front of the existing support. Temporary beams along the tunnel axis at the spring-line, spanning from the existing support behind this section to the rock in front at this section, were used to support the lining in the top heading. The next step is installation of the shotcrete and steel ribs in the opened-up bottom heading, the completing the support envelope. The final and fourth phase of the excavation is continued excavation of the bottom bench beyond this section, further loading the initial support in this section.

The conditions of the ground before excavations started is simulated by the “Initial Condition Phase”. For that phase, the initial stress condition is calculated using K0 Procedure. With the use of this procedure, pore pressure, effective stresses and state

parameters are generated with no equilibrium being warranted. The parameter used to define this initial stress conditions is the horizontal stress ratio defined above, with the singularity that only one value of K0 can be used for each material. As mentioned by Plaxis manual's, "At the end of the K0 Procedure, the full soil is weight activated".

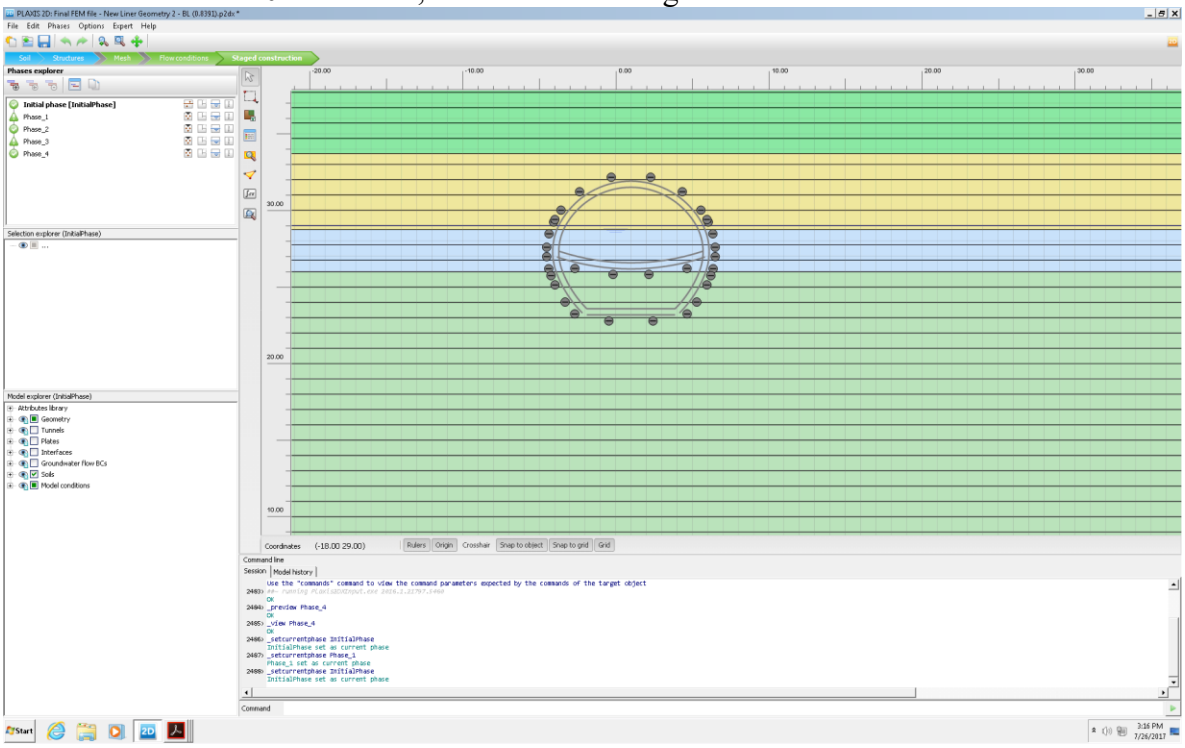

Figure 4.1: Initial Phase, with k_0 Procedure Defined to Calculate the Initial Stress Conditions

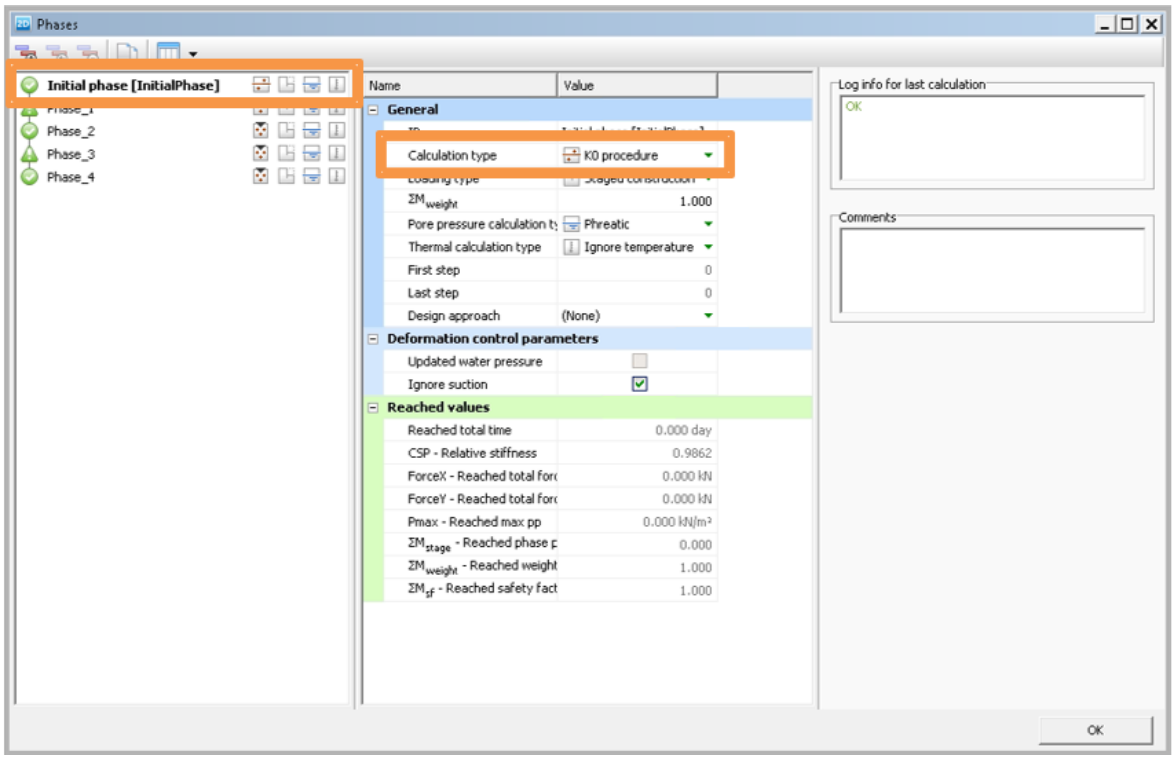

Figure 4.2: Parameters Used for Initial Phase

Once the initial stress conditions of the ground are established, the tunnel construction was modeled. The drilling and support process was defined with four phases, one excavation step followed by a support phase, then a new excavation process again and the final phase to connect the whole support system at the invert of the tunnel.

To better represent the field construction sequence, the tunnel cross section was divided in 2 sections. The division between the crown excavation and the bench was placed with an offset of about 3m from the invert of the horseshoe shape tunnel.

First the crown excavation was simulated during phase 1. The soil clusters in the crown excavations were deactivated. Deactivation soil clusters represents the removal of the soil from the field. At that moment, a 3D arching effect takes place and has to be considered in the plane strain FEM.

For FEM purposes in phase 1, the β-method (e.g., Vermeer 1993) emulates the arching effect due to the tunnel excavation advancement. Prior the tunnel is excavated, during "Initial Phase", an initial stress, pk, is acting around the area were the tunnel will be drilled. Once the excavation takes place, the initial stress condition in the area is modified; a portion (1-β) of pk is acting in the unsupported tunnel and the complement of it, β of pk, acts into the supported tunnel. This concept is considered by Plaxis 2D in the staged construction. The ΣMstage represents the βpk stress that is going to be applied at the end of the phase for the supported tunnel. There are several manners to estimate β, for this analysis, the equation proposed by Panet (1995) in the stress relief method was used. This equation is a function of the span between the support and the tunnel face, the excavation radius and the initial stress condition in the ground. Figure 4.3 illustrates the concept explained above.

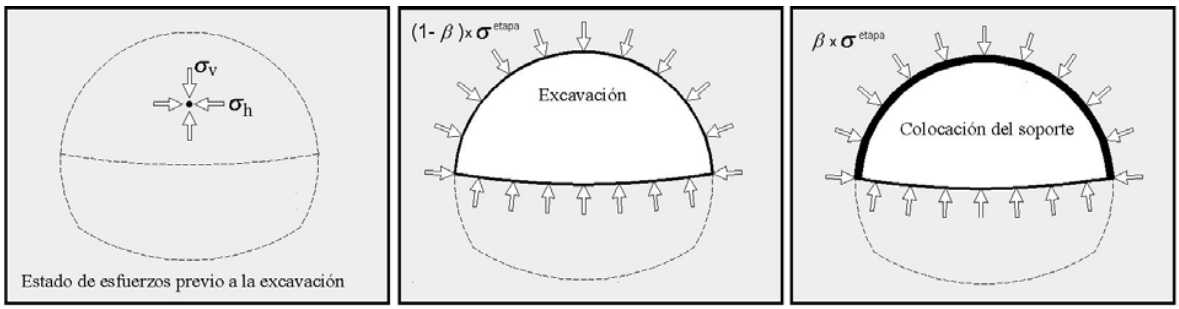

Figure 4.3: β Method Used to Analyze the 3D Arching Effect (From Manual de Diseno y Construccion de Tuneles de Carretera)

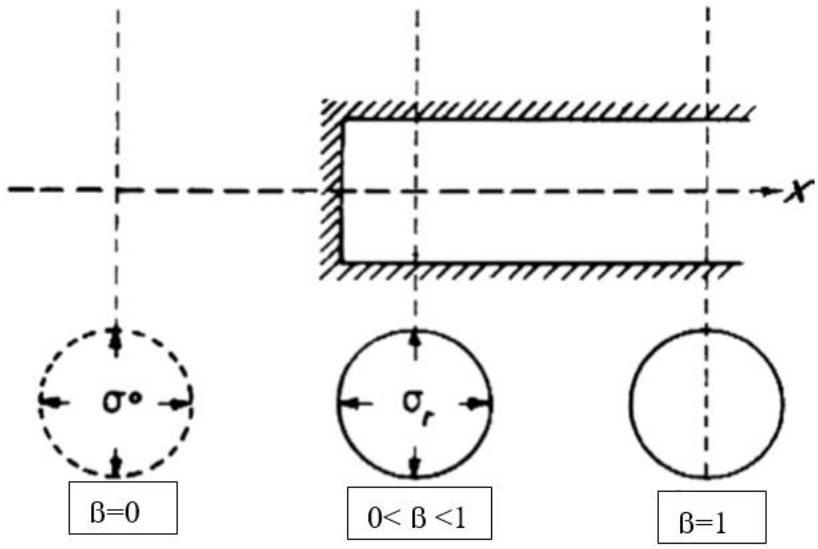

Figure 4.4: Values of β for Different Stages During Construction (From M. Karakus 2006)

Figures 4.5 and 4.6 represent the excavation of the crown cluster, phase 1. A value of β equal to 0.1609 was adopted to represent the 3D arching effect in the FEM.

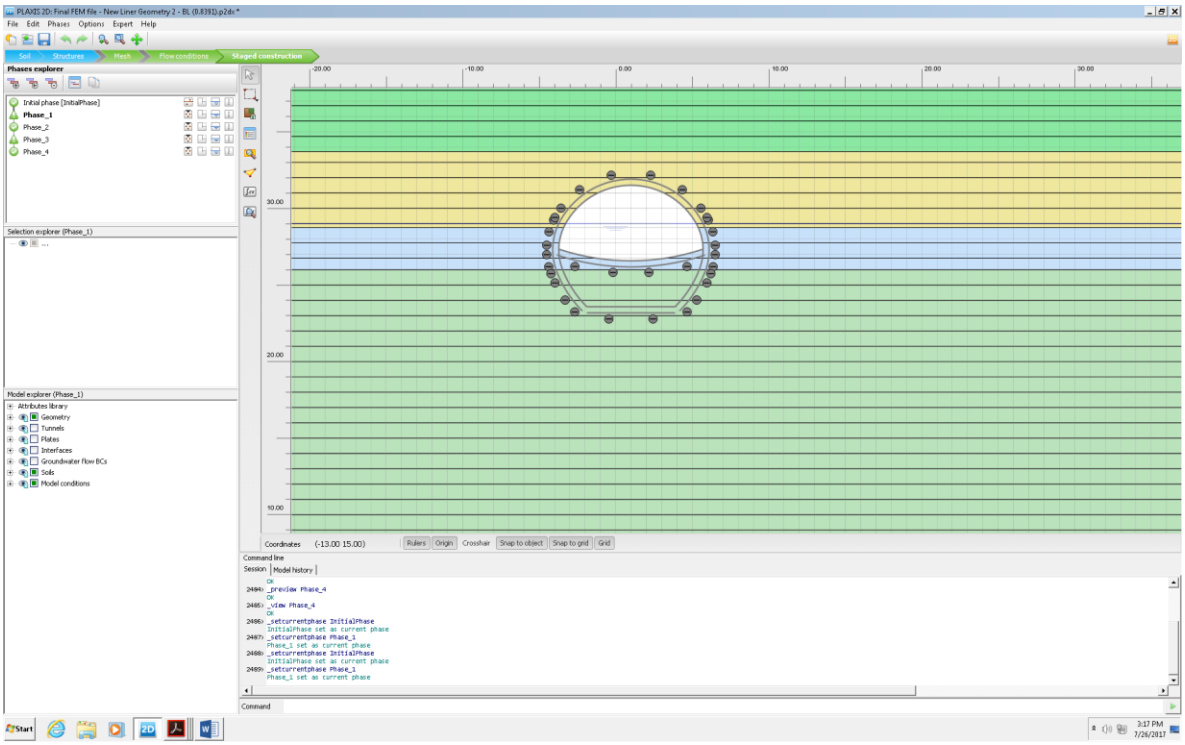

Figure 4.5: Phase 1, Soil Was Deactivated in the Crown Cluster to Simulate the Excavation that Took Place in the Field

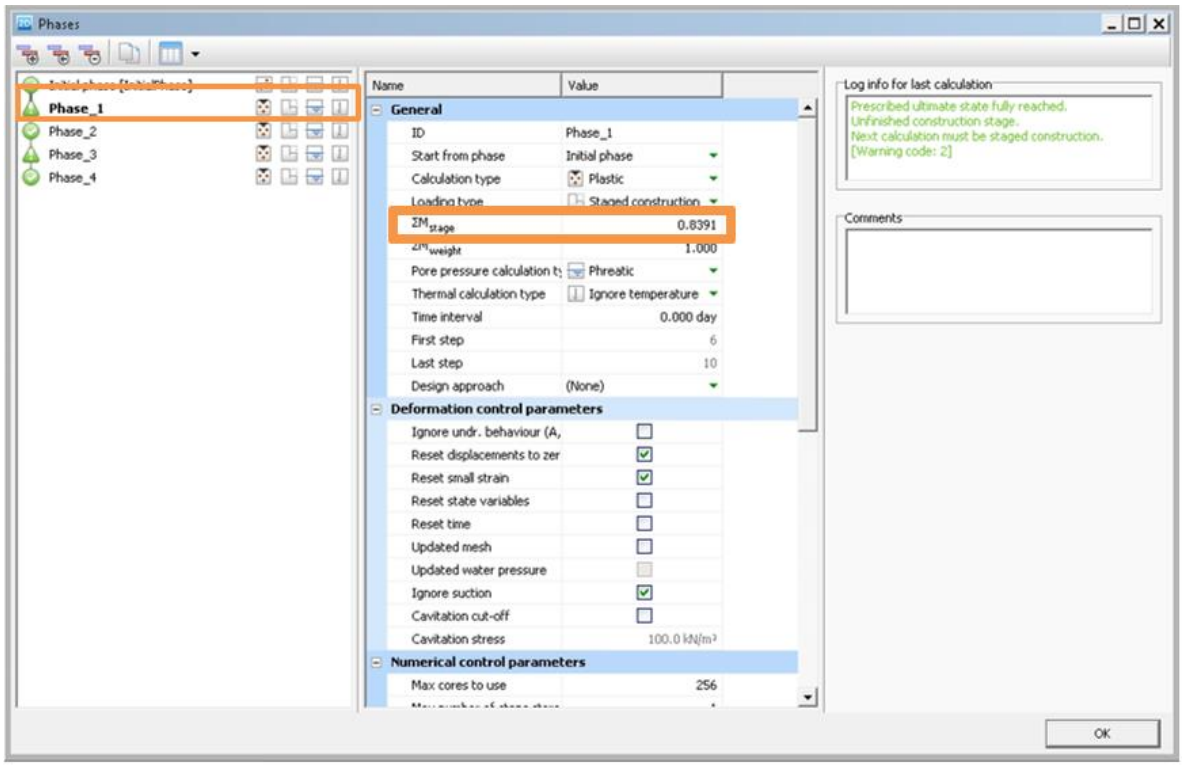

Figure 4.6: Plaxis Input Parameter in Phase 1 to Take into Account the Span Between Tunnel Face and Placement of Liner

After the excavation of the top cluster, the liner was placed. In the field, W8x15 steel beams were used as steel ribs placed distant of 1.22 m between each other along the tunnel axis. Furthermore, 15 cm of Poly Fiber Reinforced Shotcrete was placed. The steel ribs were resting on steel beams place at the bottom of them in order to avoid significant settlements when excavating the bench. This situation was simulated in the FEM by activating a liner plate around all the tunnel but the invert. The plate that extends into the bench soil, emulating the function of the steel beams used to support the ribs.

Phase 2 excavation of the top heading beyond the newly placed support was then simulated by removing the effect of 3D arching (i.e., β of 1). Figures 4.7 to 4.9 illustrate the procedure followed in the FEM.

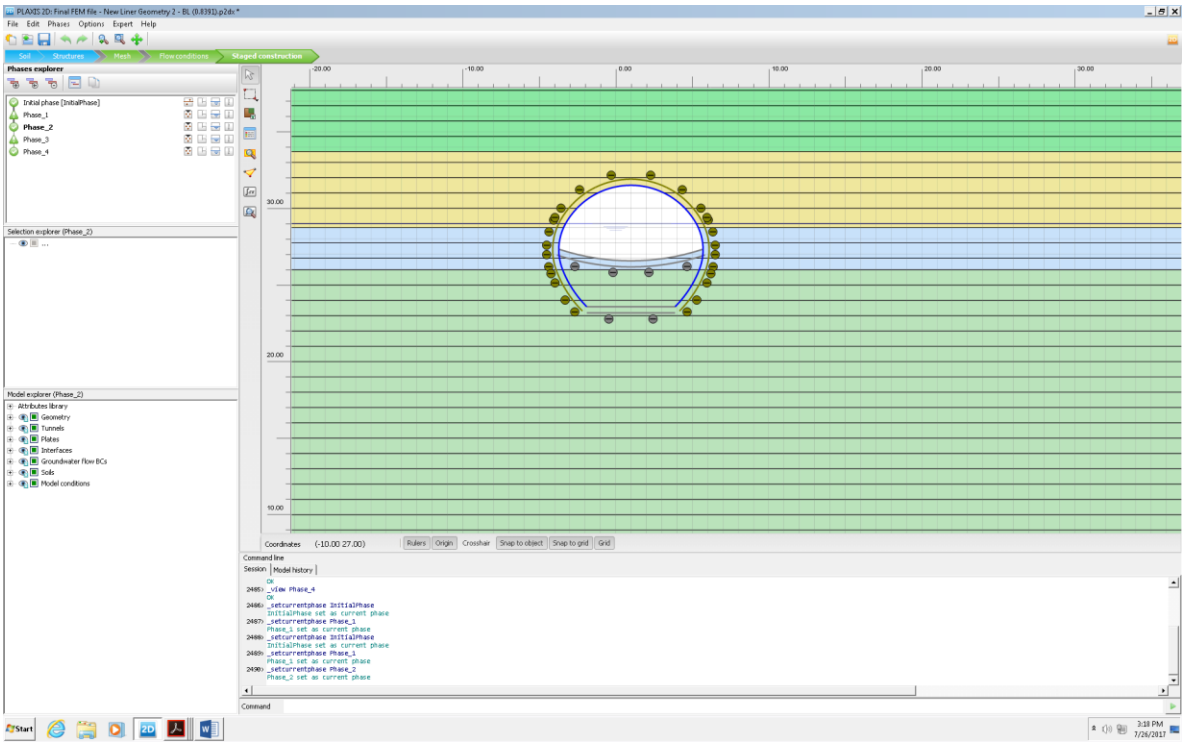

Figure 4.7: Simulation of Liner Installation by Activating the Liner Plate in the FEM

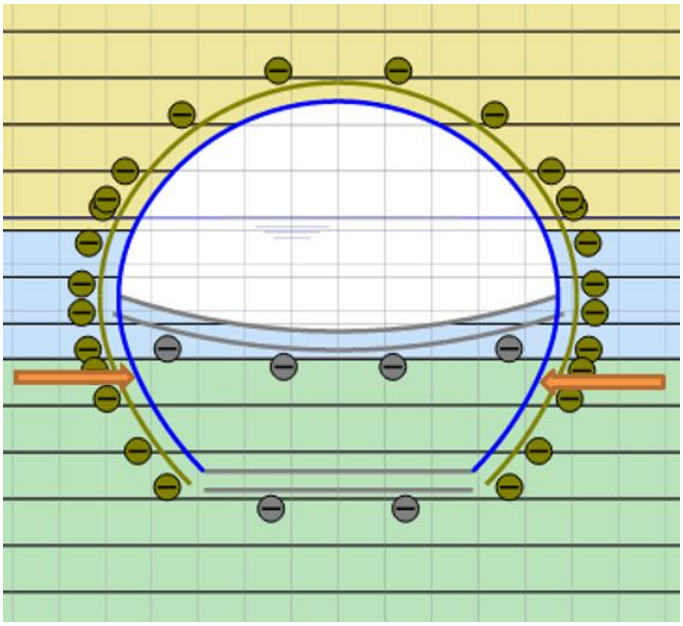

Figure 4.8: Orange Arrows Indicates the Liner in the Bench Soil Emulating the Steel Beams Acting as Footing of the Steel Ribs During Construction

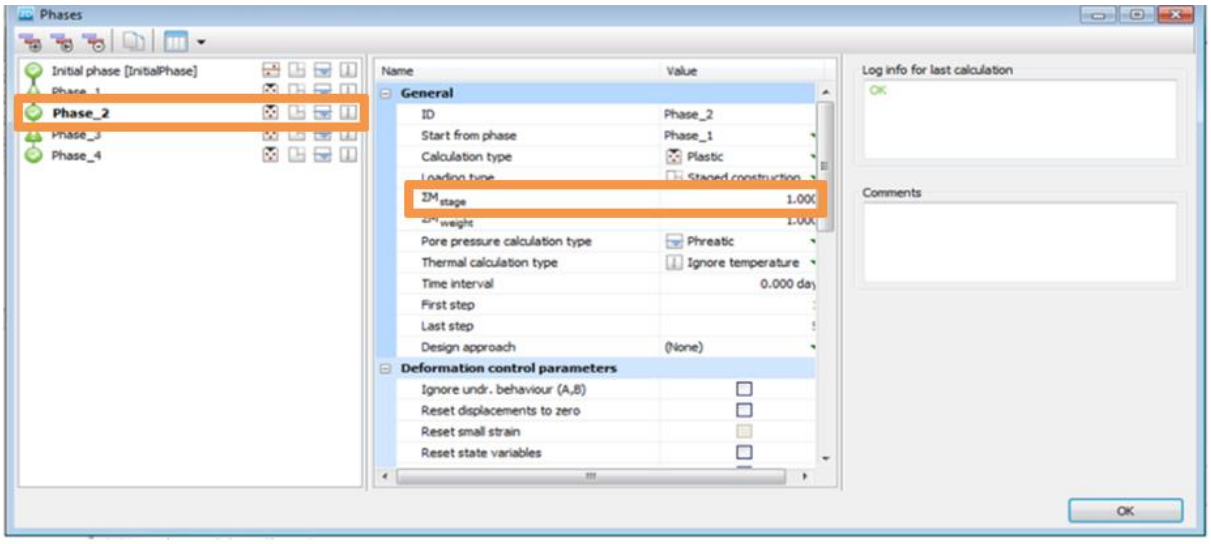

Figure 4.9: Phase 2 General Parameters

The excavation of the bench was carried out in phase 3. During this phase, the soil clusters of the bench were deactivated in the FEM. Figure 4.10 and 4.11 illustrates this phase and the parameters used to simulate it. During phase 3, no additional placement of support was considered in the FEM since it was completely placed before phase 2. At the completion of phase 3, the liner was closed by the incorporation of the liner at the invert of the tunnel. The mechanical characteristics of the liner activated at the invert match the mechanical characteristics of the rest of the liner.

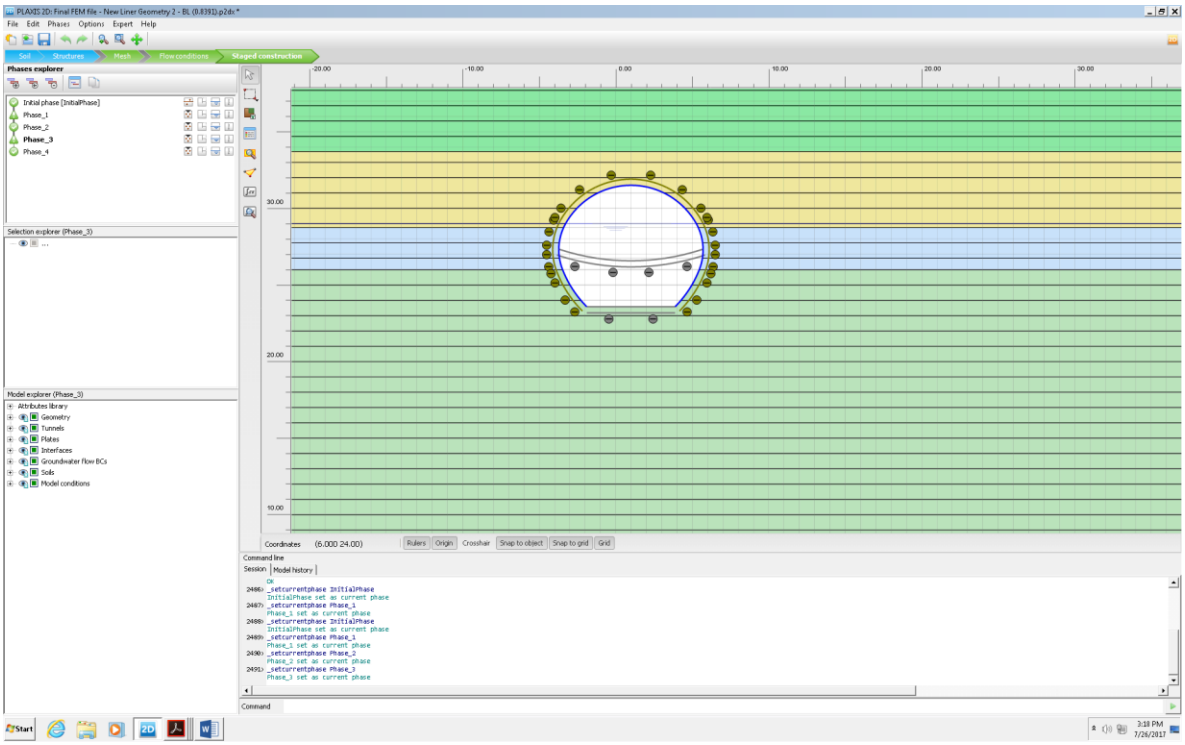

Figure 4.10: During Phase 3, the Soil Clusters at the Bench were Deactivated

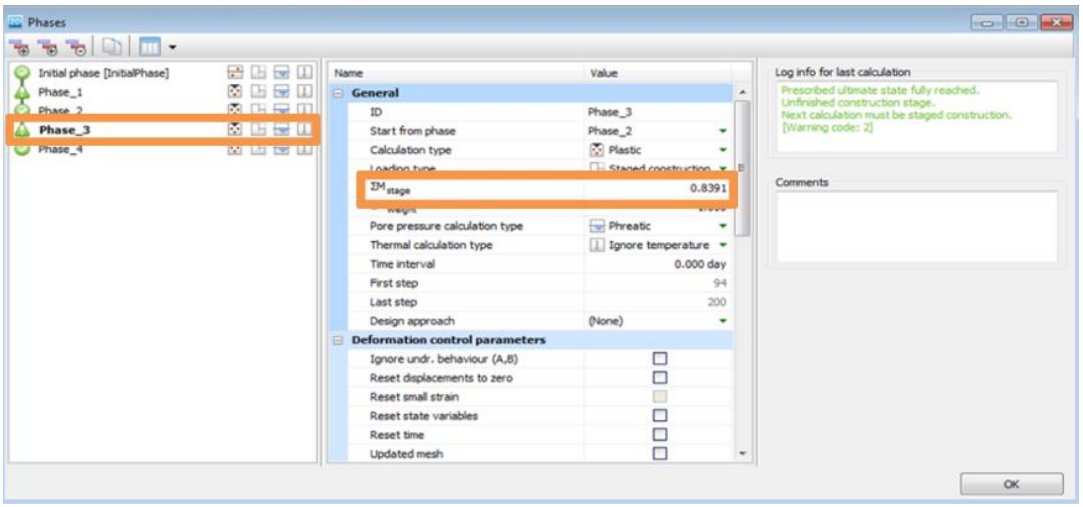

Figure 4.11: Phase 3 General Parameters

The construction sequence was completed with the introduction of phase 4. During the last phase of the FEM the bottom bench excavation beyond the newly placed support was simulated by removing the effect of 3D arching (i.e., β of 1). Figure 4.12 to 4.14 shows in detail phase 4.

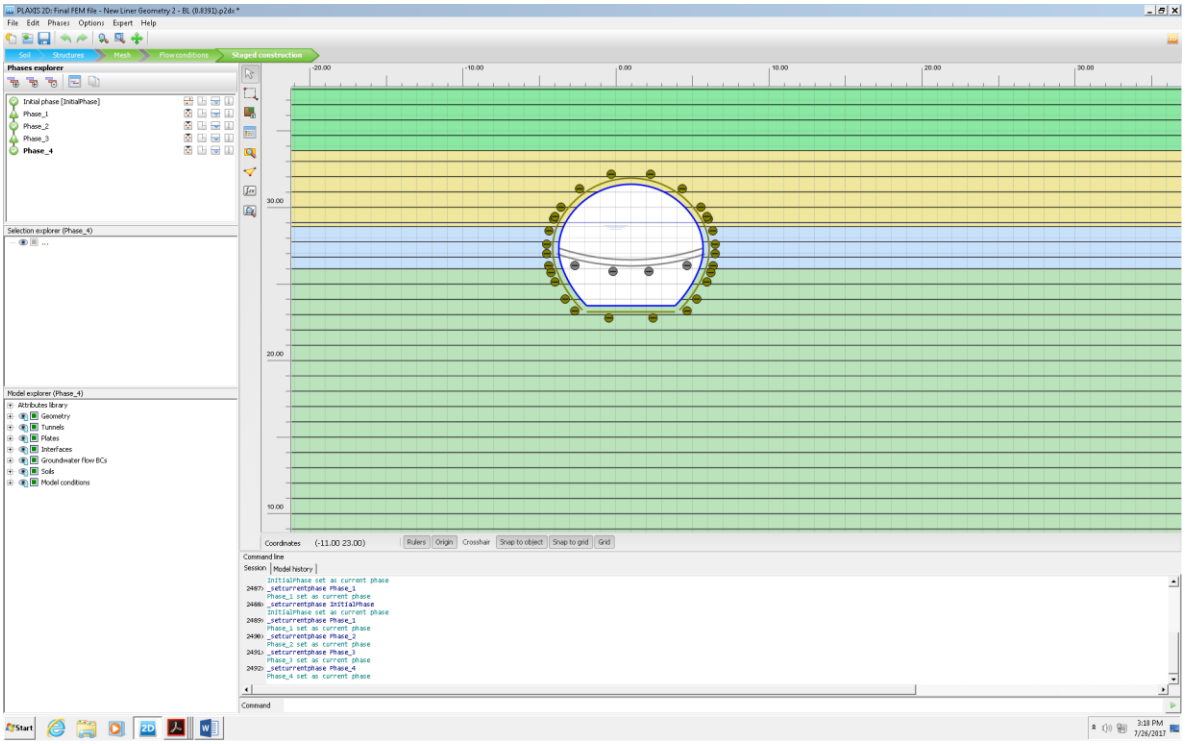

Figure 4.12: Phase 4 Represents the Stage of the Construction Sequence

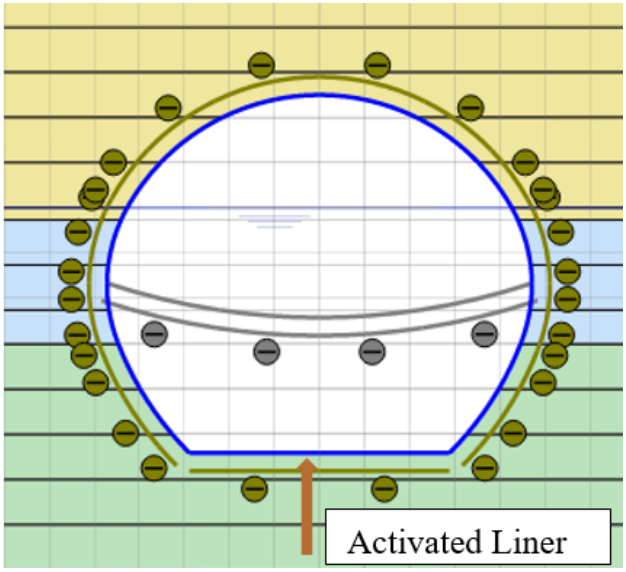

Figure 4.13: Orange Arrow Indicated the Activated Liner at the end of the Construction Sequence

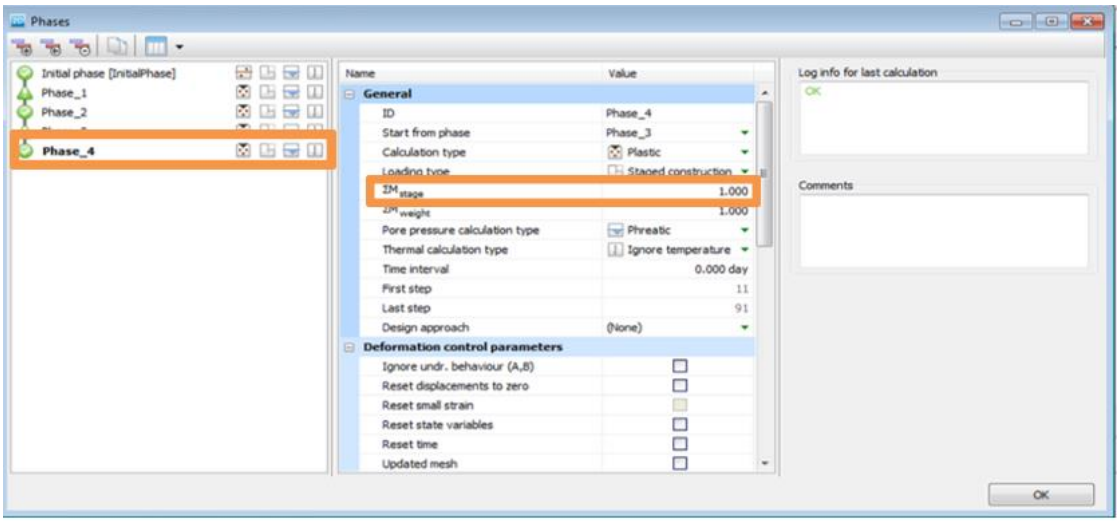

Figure 4.14: Phase 4 General Properties

4.2 RESULTS

Figure 4.15 through 4.20 presents the results from the finite element analysis at the moment the total cross section was excavated and all the support system was placed (i.e., the completion of phase 4 excavation).

In Figure 4.15 it is possible to see how the total displacements of the tunnel support increases as approaching the invert. At the invert, there is also some inward movement expected in the form of heave. The maximum total radial displacement expected according to the FEM is less than 2cm.

According to Figure 4.16, little vertical displacement is expected in the tunnel lining walls unless in the proximity with the invert. The above-mentioned heave of the invert is where the larger vertical displacements are expected.

On the other hand, when analyzing the horizontal displacement result from Figure 4.17, all of them take place along the walls of the tunnel. The magnitude of the horizontal displacements as is expected, increases with the proximity to the invert.

The liner is all subjected to compressive (negative) thrust, as expected. Maximum thrust is found at the crown while minimum values are at the spring-line vicinity, as presented

by Figure 4.18. This pattern reflects the initial stresses in the ground with $K_0 > 1$. Figure 4.19 presents the shear results while Figure 4.20 presents the bending moments.

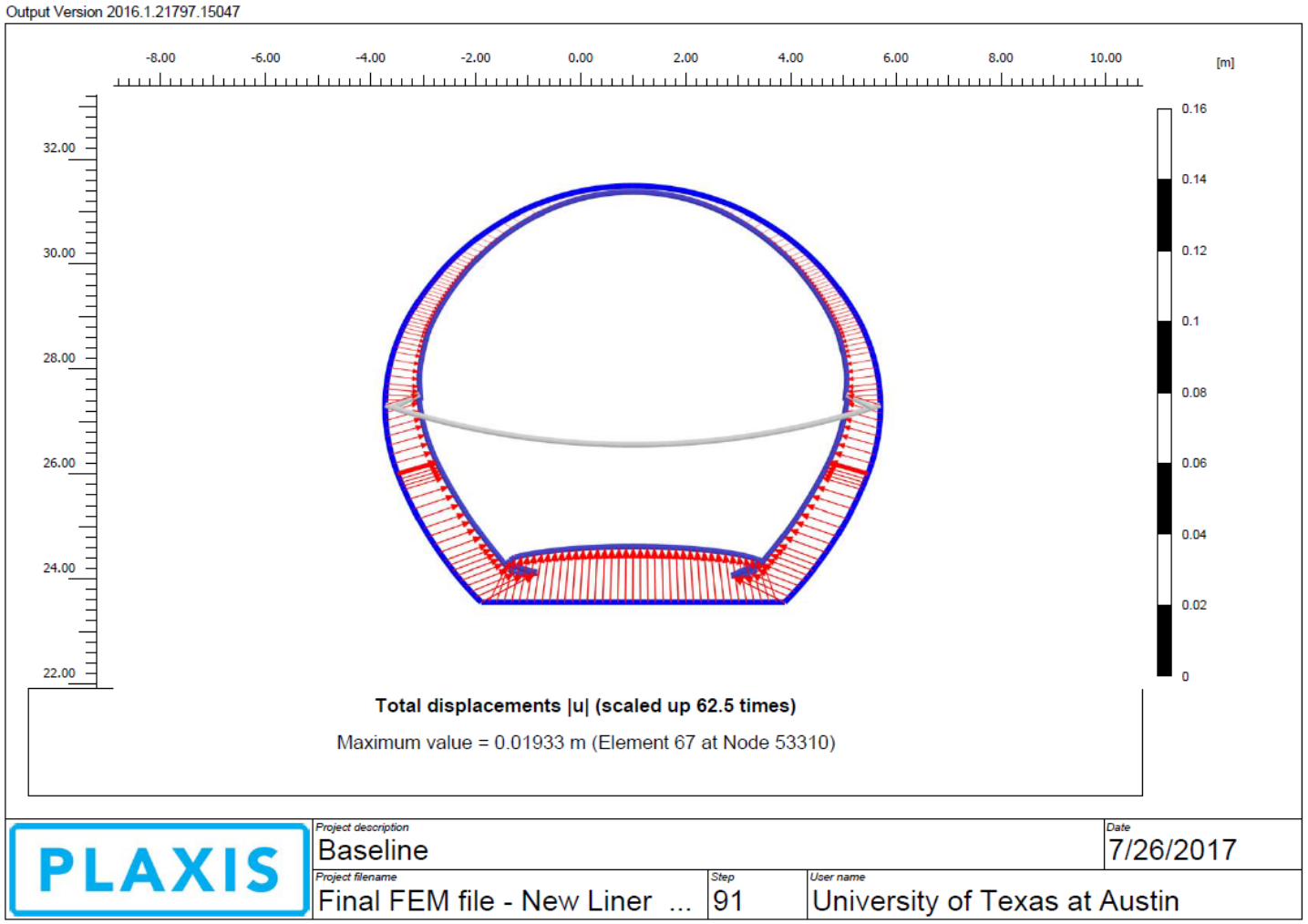

Figure 4.15: Total Displacements

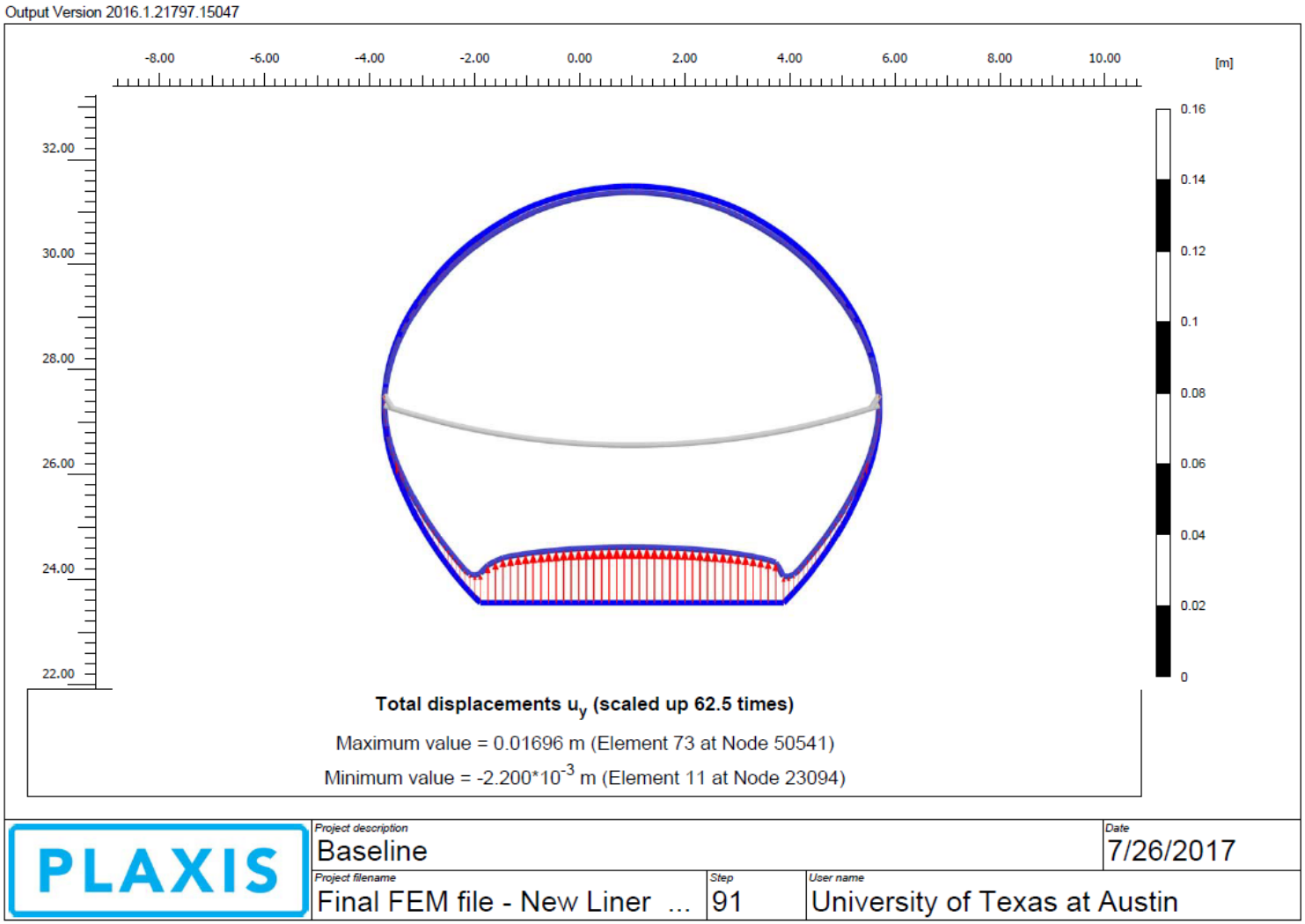

Figure 4.16: Vertical Displacements

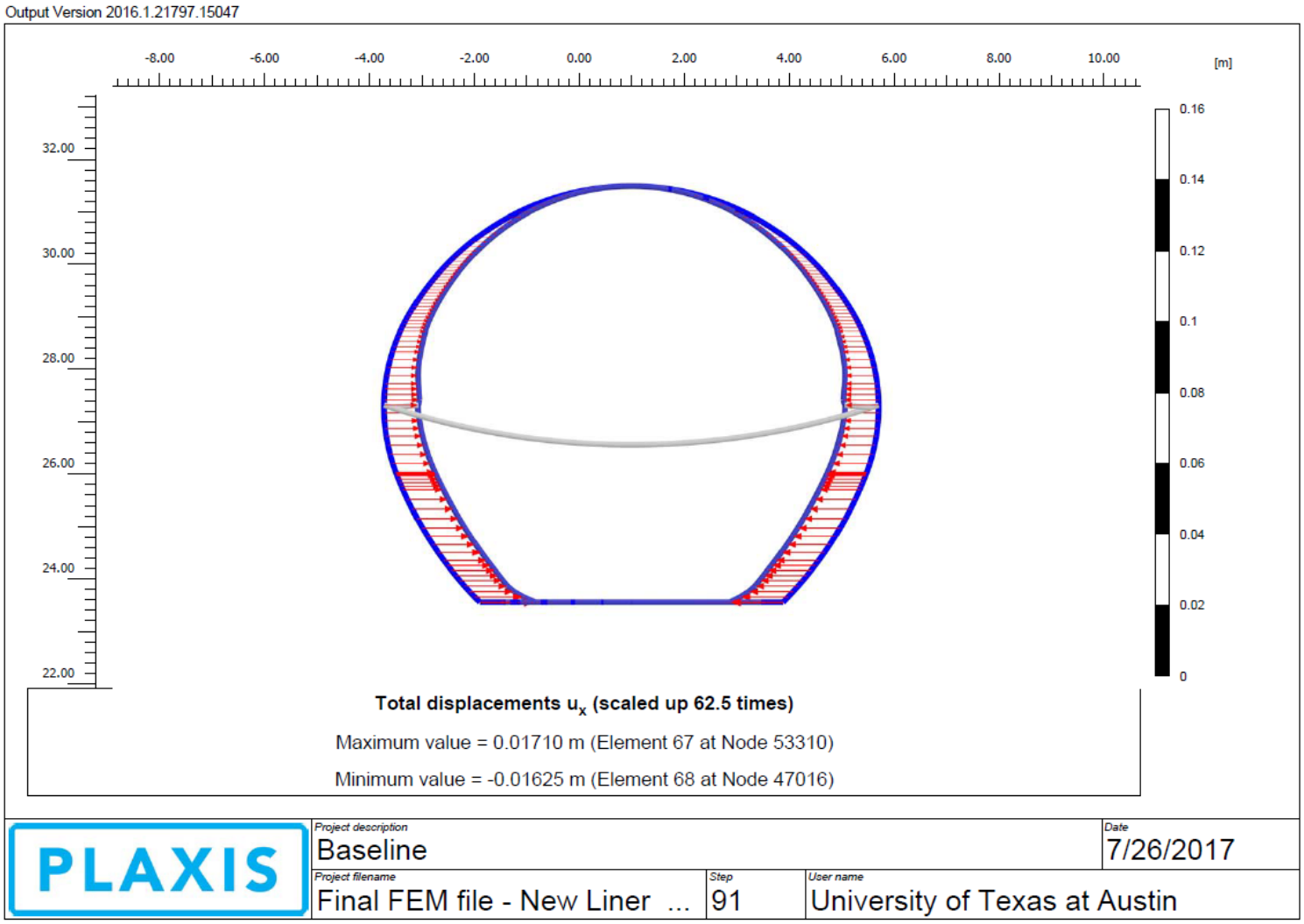

Figure 4.17: Horizontal Displacements

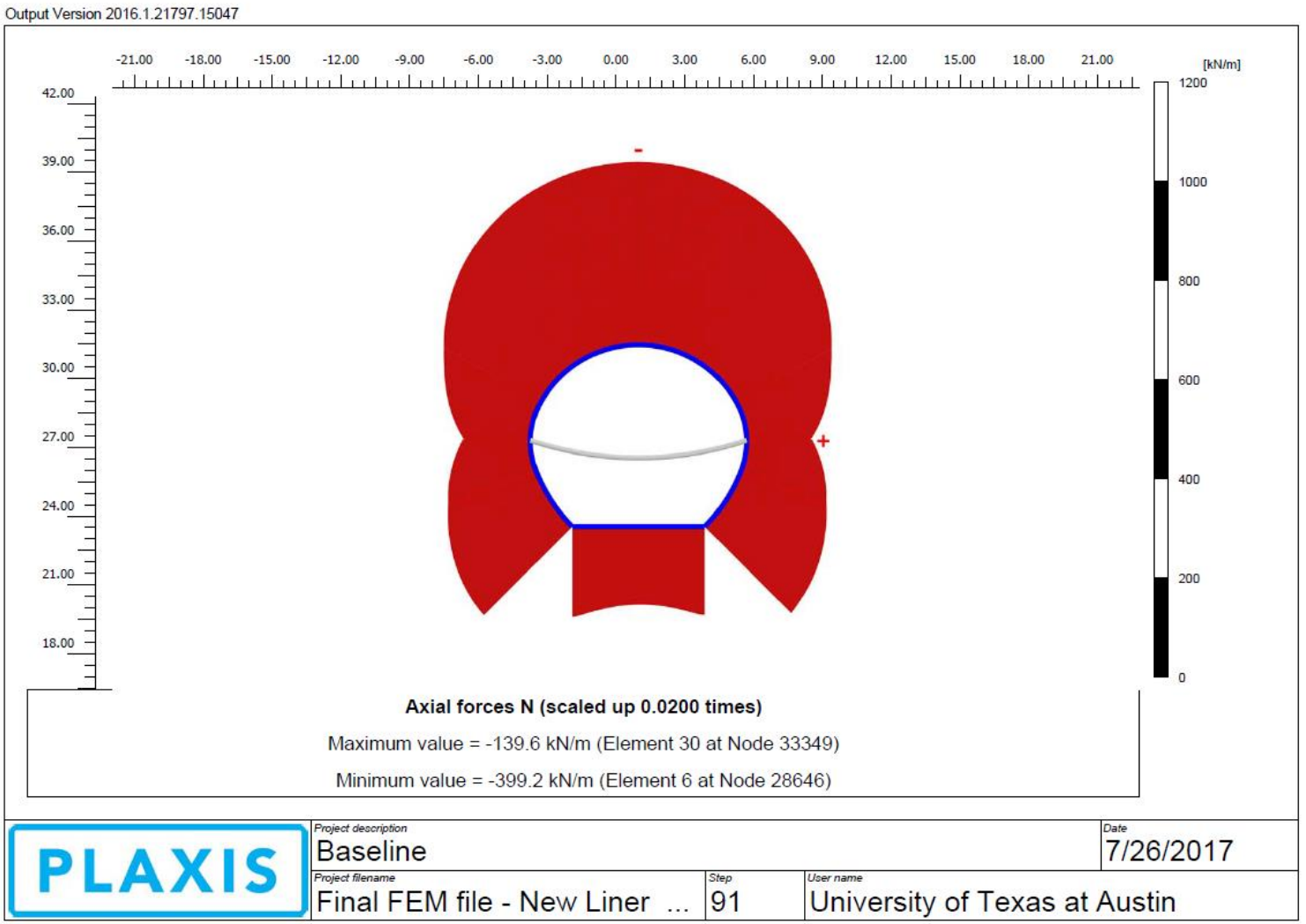

Figure 4.18: Axial Forces Along the Liner

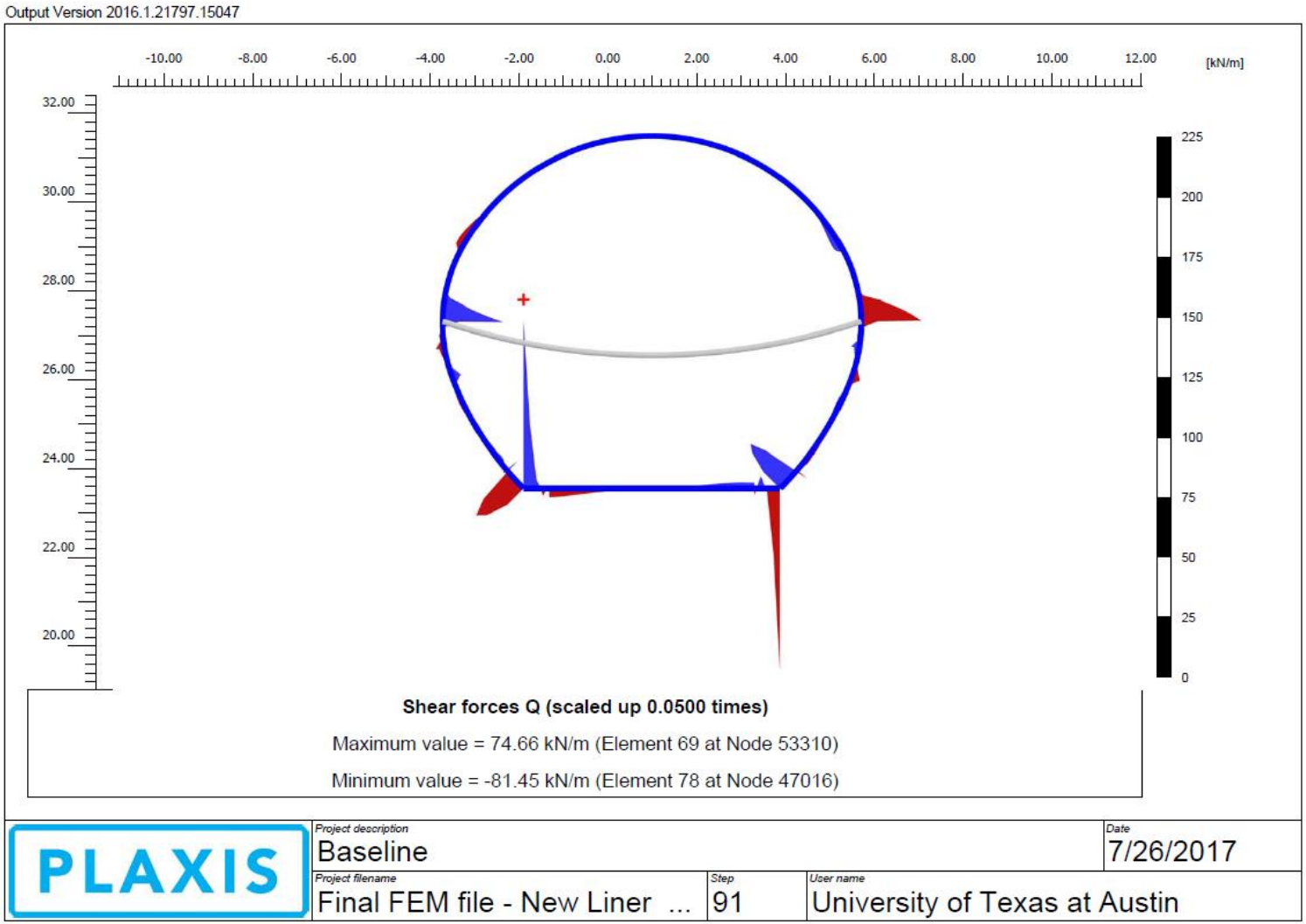

Figure 4.19: Shear Forces

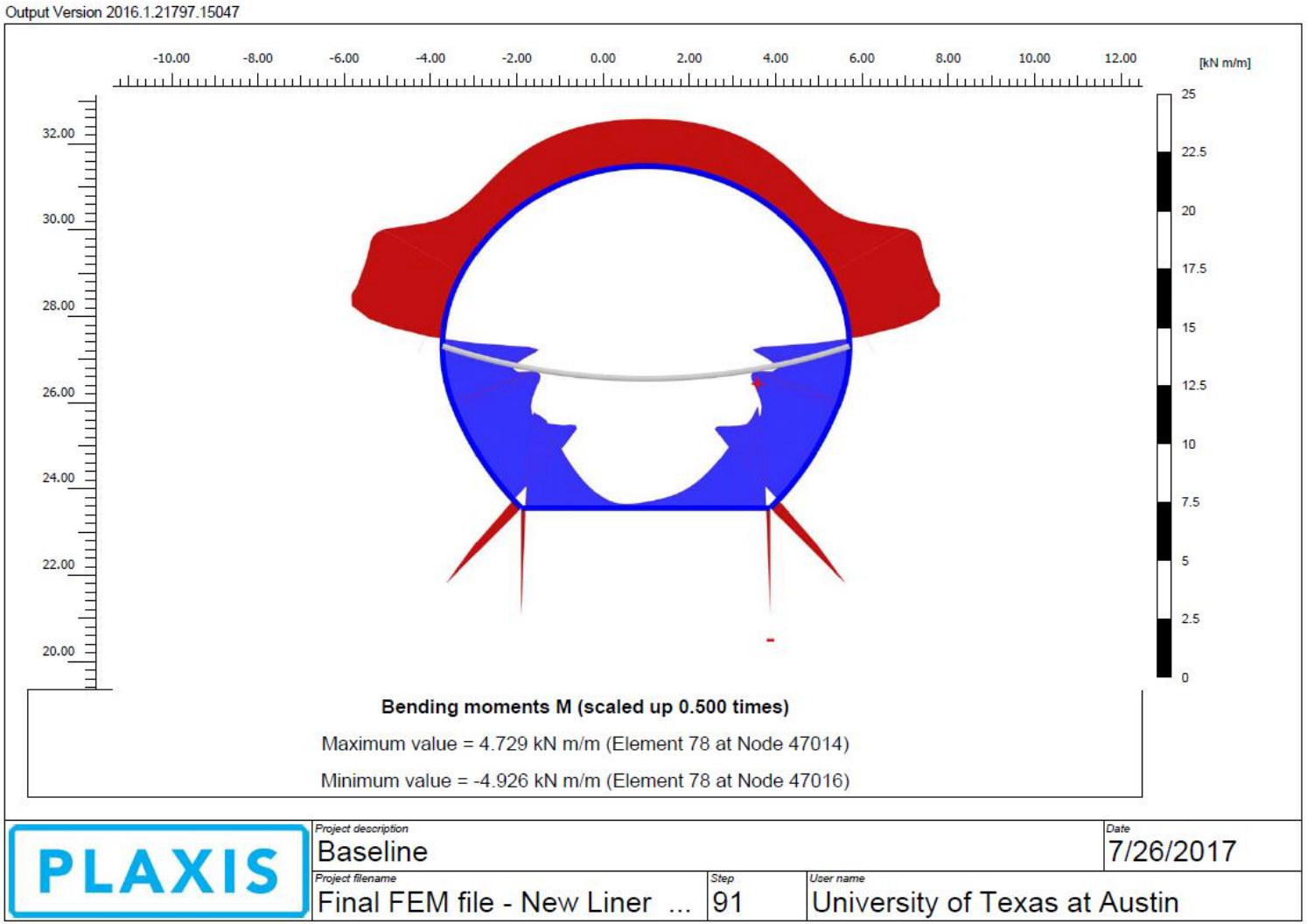

Figure 4.20: Bending Moments

Table 4.1 presents average values of thrust and normal pressure on the tunnel wall. The data corresponds to the selected points at the crown and the spring-line at the end of phase 2, 3 and 4. An interesting result is that the forces on and in the liner decrease with additional excavation after phase 2 (excavation of the top heading after the initial support is placed). This result occurs because the liner is not closed until after the phase 3 excavation, meaning that it becomes more flexible and sheds load to the surrounding ground. Once it is closed at the end of phase 3, the liner then takes on additional load when the full excavation (phase 4) is completed (Table 4.1).

As a check of the FEM calculations, these results are compared with the design calculations (Lachel 2012). While the comparison is not exact because the geometry of the support system was modified between design and construction (and the FEM results are for what was actually built), the results are reasonably comparable. The differences between stresses and forces in the crown versus springline and the magnitudes of the radial stresses and the thrusst at the end of phase 4 are similar.

	Phase 2		Phase 3		Phase 4	
	Radial Stress	Thrust	Radial Stress	Thrust	Radial Stress	Thrust
	kN/m2	kN/m	kN/m2	kN/m	kN/m2	kN/m
Crown	-116	-532	-83	-375	-88	-399
Springline	-149	-516	-73	-141	-78	-150

Table 4.1: Summary of the FEM results

Chapter 5. Waller creek tunnel in situ data

This chapter has the intention of provide information about the actual tunnel construction in the field. The stress cells used in the Waller Creek Tunnel to measure in situ radial and tangential stress are described in this chapter. The measurements are then presented.

5.1 Stress Cells

During the construction process stresses were recorded. For that purpose, special stress cells developed to use be placed in shotcrete for conventional tunneling construction method were used. They were placed after phase 1, and intended to measure radial and tangential stresses in the liner during phases 2, 3 and 4 of excavation.

The stress cells design consists of 2 peripherally welded rectangular plates with a gap in between them (Geokon 1993). This thin gap is filled with hydraulic oil in order to experience changes in stress conditions. Those variations in pressure are measured with a vibrating wire that is connected to the gap between the plates with a pressure tube.

To avoid possible errors due to the creation of gaps between the stress cells and the concrete after the entire cure process has taken place and concrete has cooled off completely, a pinch tube was incorporated to inflate the cell and put it in contact again with the concrete.

5.1.1 Installation

Those cells are intended to measure both, tangential stress and radial stress. According to that, each cell has a specific position.

Those cells intended to measure tangential stress, must be installed at the crown and spring-lines in a parallel position to the liner cross section. Special care must be taken when spraying the shotcrete to avoid shadow zones.

On the other hand, the cells used to measure radial stress are installed in interface between the ground and the liner, having of the flat surfaces in contact with the ground. Before the installation of the cell, the ground surface has to be prepared to provide proper

conditions for the cell-ground contact. Moreover, “the cell must be gripped firmly” with the help of nails as specified by Geokon in the Instruction Manual (Geokon 1993).

5.1.2 Pressure Calculation

When reading the cells in the field, the raw data obtained is made out of digits that need to be converted into pressure to make it able to interpret. This transformation is possible thanks to the following formula provided by Instruction Manual of Geokon:

Pressure= (Current Reading – Initial Reading) x Calibration Factor.

The Initial Reading is the one obtained after the cells were installed and before the top heading was excavated further (i.e., between phase 1 and phase 2 of excavation).

5.2 Measured Stresses

With the use of the stress cells mentioned above placed at the crown and spring-line of different stations, in situ stresses were measured during construction. Some of the data is presented in Figures 5.1 through 5.4. The construction specification included an “Action Level,” which triggered additional monitoring, and a “Maximum Level,” which triggered remedial action. The Action Levels are similar to maximum values predicted based on the design calculations (Lachel 2012).

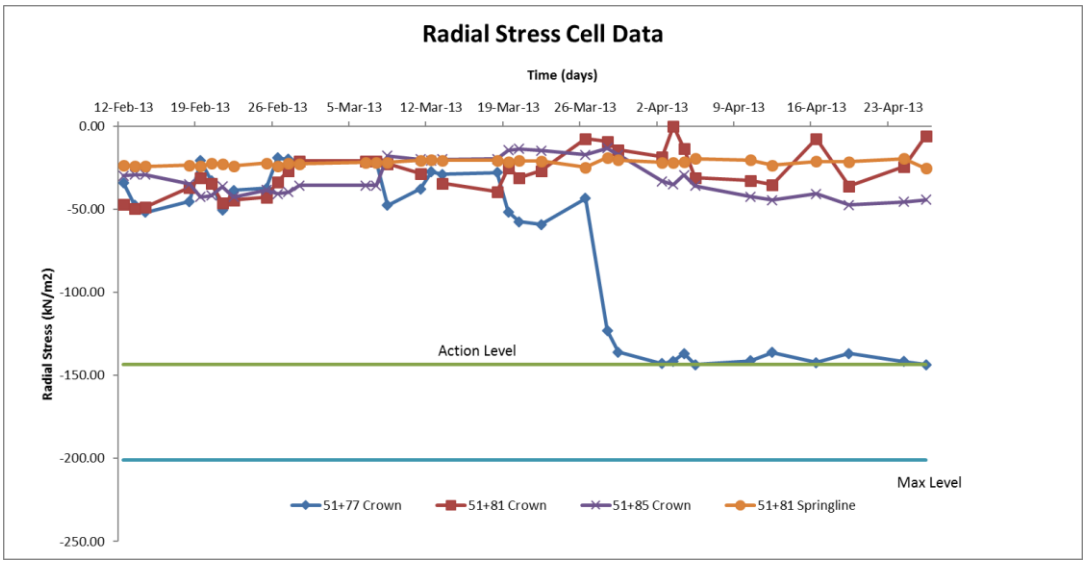

Figure 5.1: In Situ Radial Stress Cell Data in psi at Stations 51+77; 51+88 and 51+81

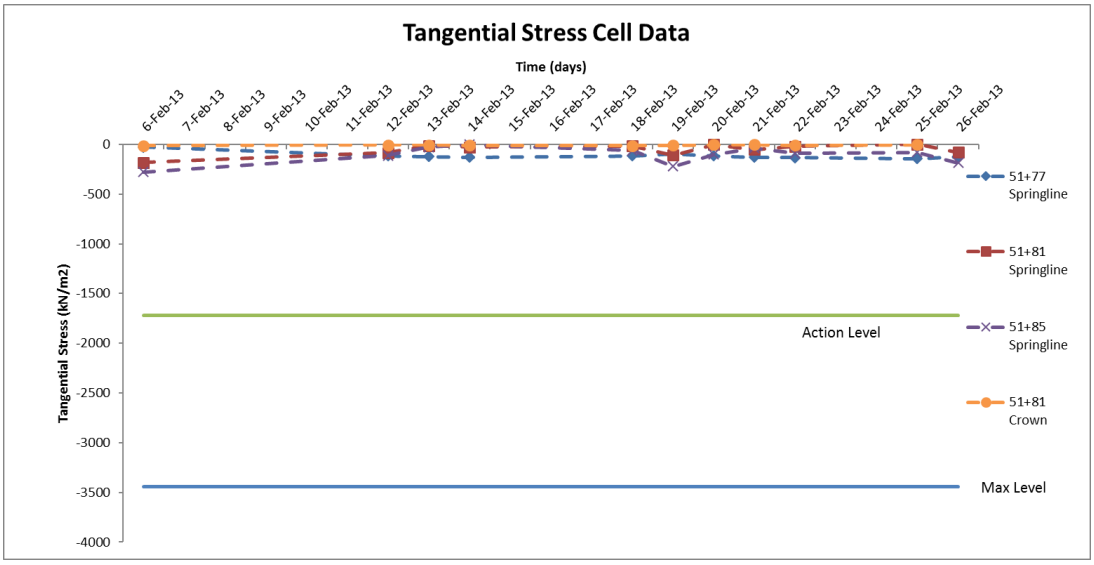

Figure 5.2: In Situ Tangential Stress Cell Data at Stations 51+77; 51+88 and 51+81

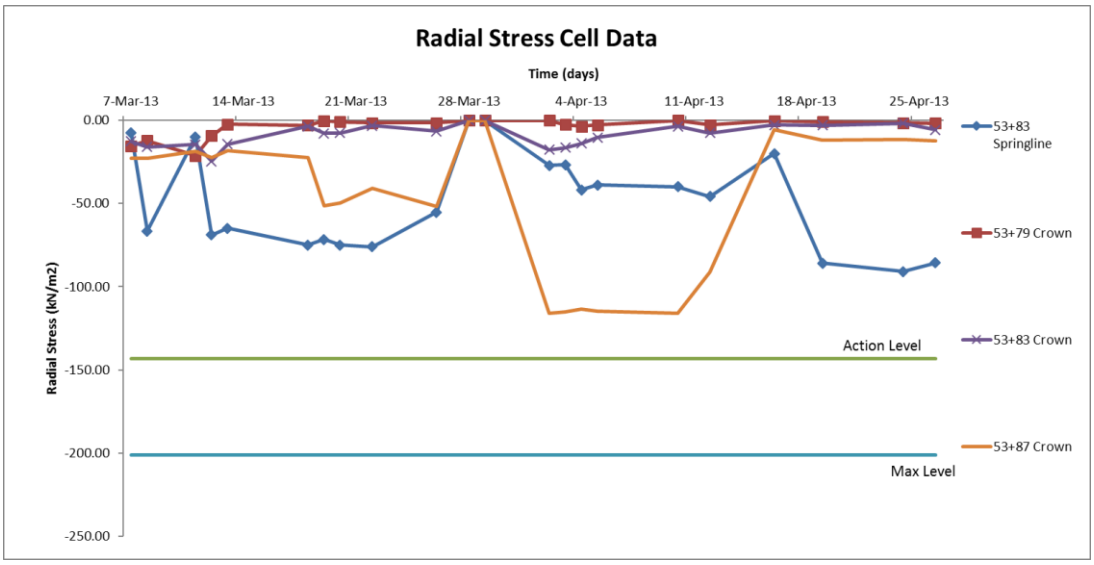

Figure 5.3: In Situ Radial Stress Cell Data at Stations 53+83; 53+79 and 53+87

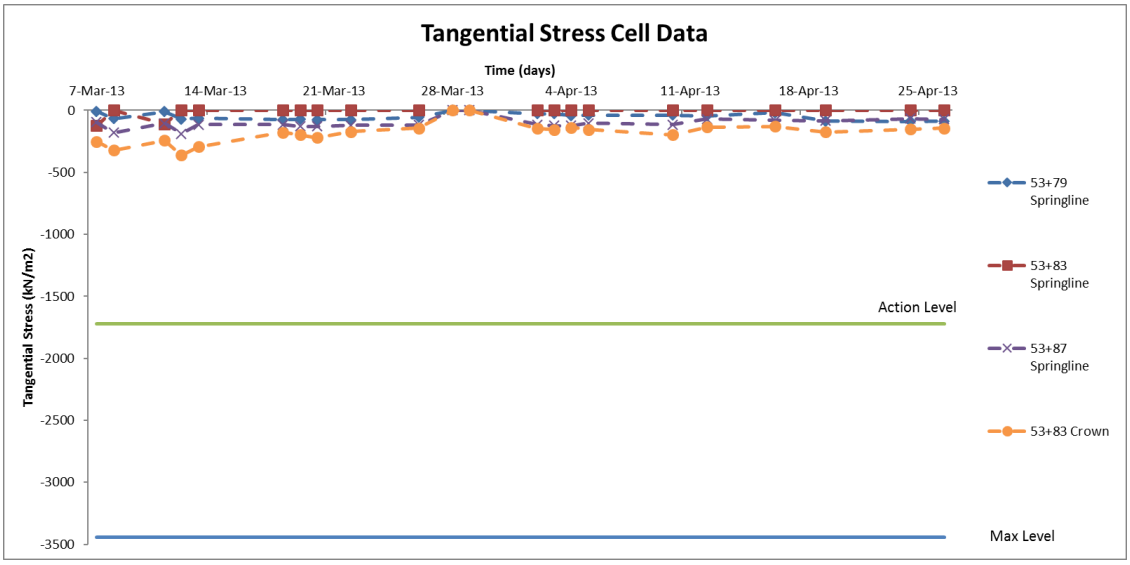

Figure 5.4: In Situ Tangential Stress Cell Data at Stations 53+83; 53+79 and 53+87

The field data for both radial and tangential stresses are generally well below the Action Levels, particularly the tangential stresses. The ratio of the measured tangential stresses to the radial stresses is between 10 and 20. Last, both the radial and tangential stresses tend to decrease with time (i.e., with further excavation from phase 2 to phase 4).

Chapter 6. Comparison Between Waller Creek Tunnel In-Situ Data and FEM Results

This chapter presents a comparison between the FEM predictions and the field measurements. Figure 6.1 shows radial stresses predicted by the FEM analyses for phases 2 and 3, and Figures 6.2 and 6.3 compare these predictions with the measurements. The measurements are about one-half of what is predicted

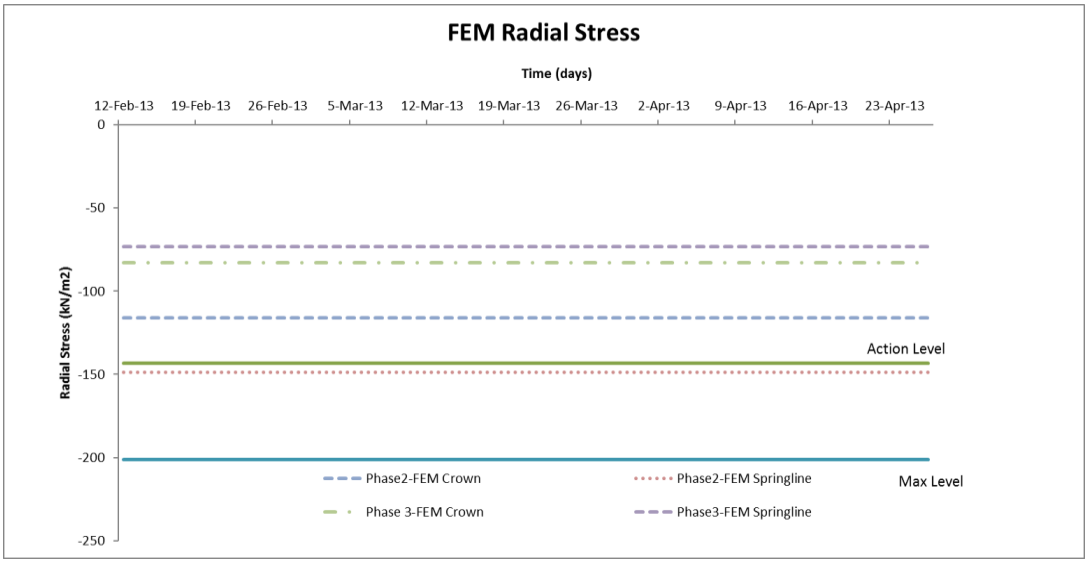

Figure 6.1: FEM Radial Stress Results

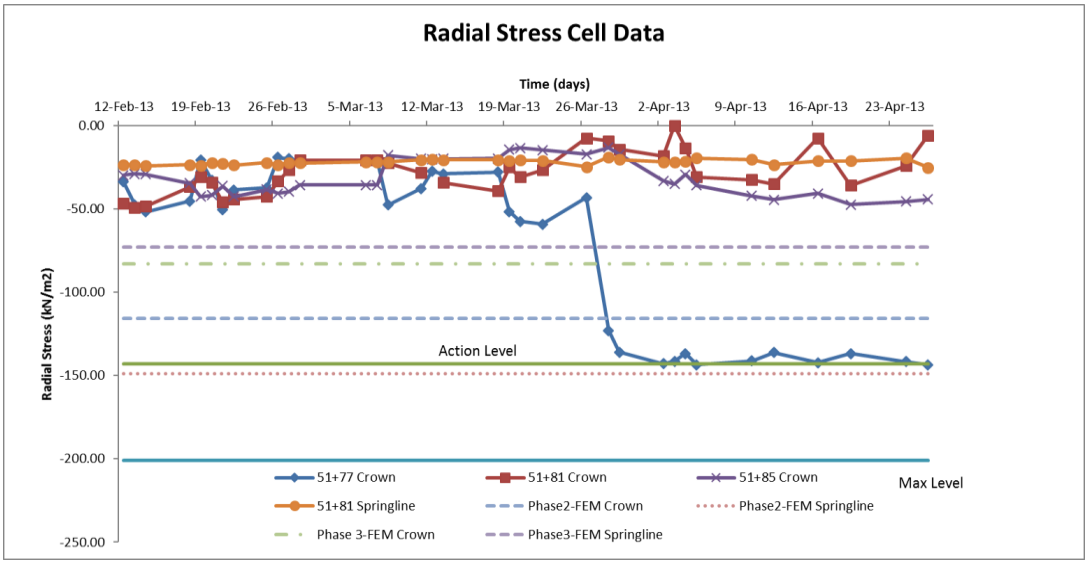

Figure 6.2: Stations 51+77, 51+81, 51+85 and FEM Radial Stress

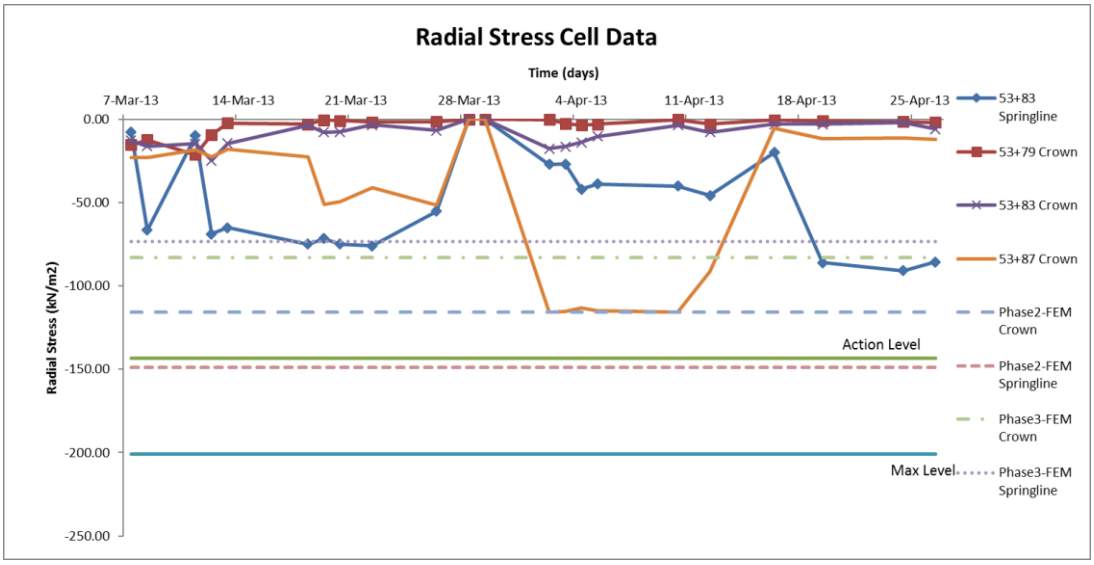

Figure 6.3: Station 53.83, 53.79, 53.87 and FEM Thrust

Figure 6.4, presents the FEM thrust results for phase 2 and phase 3, while Figures 6.5 and 6.6 compare these predictions with the field measurements. The measurements in all cases are well below the FEM results, as much as five times smaller.

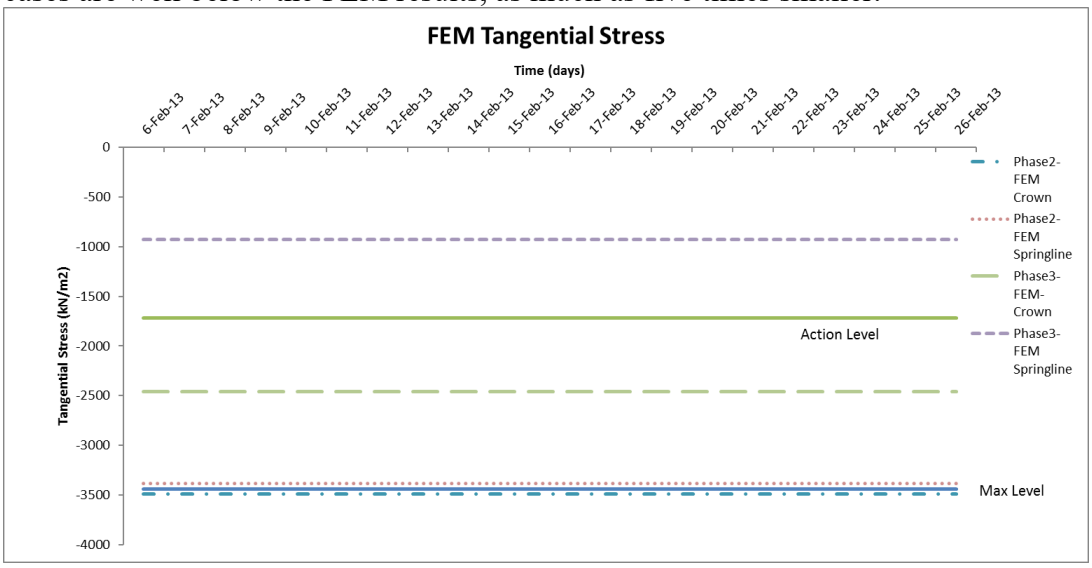

Figure 6.4: FEM Tangential Stress

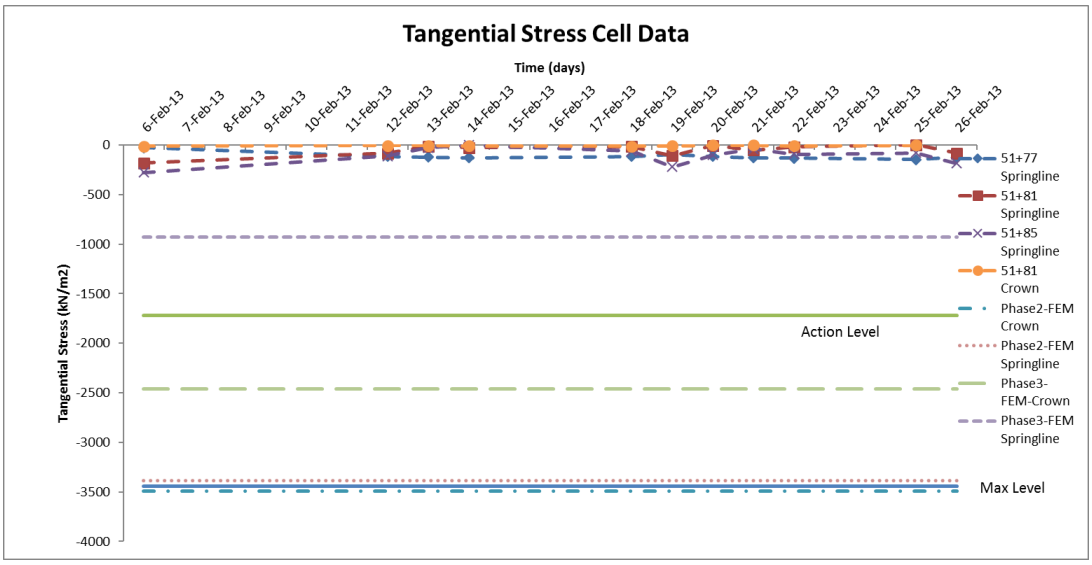

Figure 6.5: Station 51+77, 51+81, 51+85 and FEM Thrust

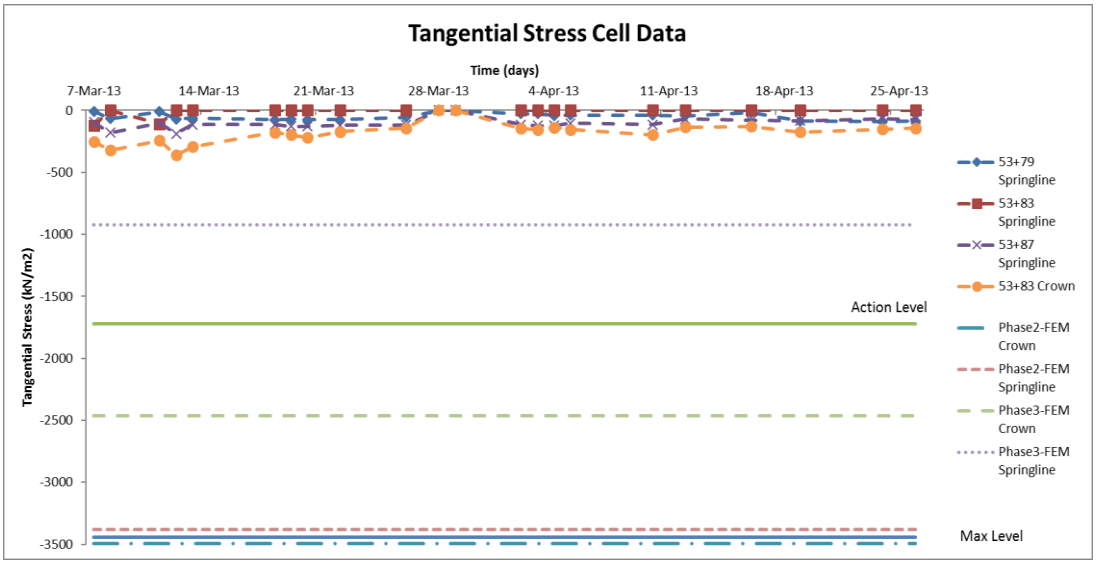

Figure 6.5: Station 51+77, 51+81, 51+85 and FEM Thrust

One possible explanation for the smaller measured stresses is that the ground may be stiffer than assumed in the FEM analyses. Figure 6.7 and 6.8 shows the FEM results obtained when using larger Young's modulus 20 times larger than those adopted from an initial analysis. In this case, the predicted radial stresses are closer to the measurements but still greater by about 50 percent greater. However, the predicted tangential stresses are still

significantly greater than what was measured. One possible explanation for the discrepancy is that the stress cells did not have intimate contact with the liner.

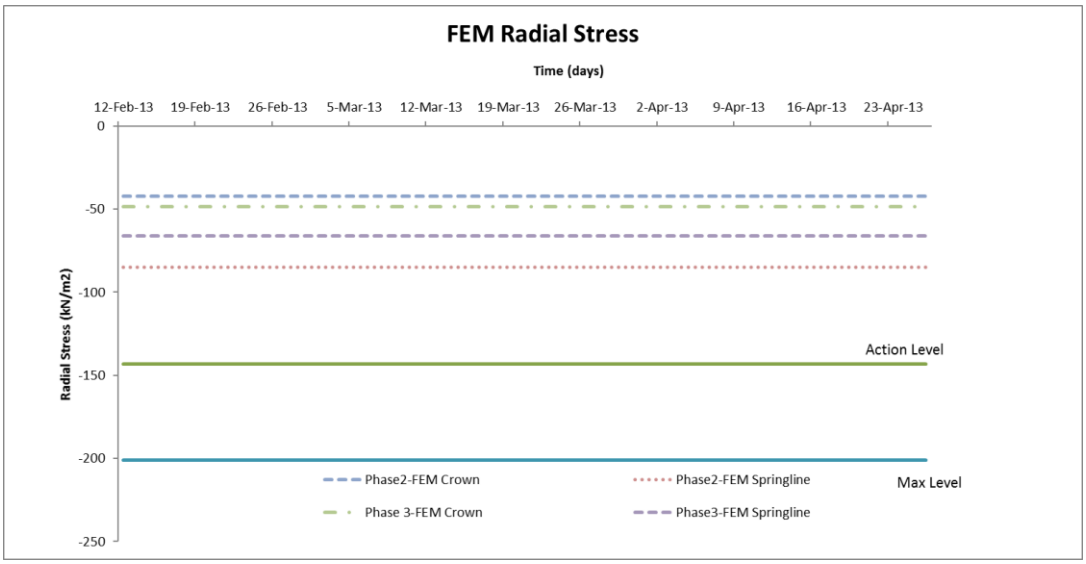

Figure 6.6: FEM Radial Stresses when Using Stiffer Ground

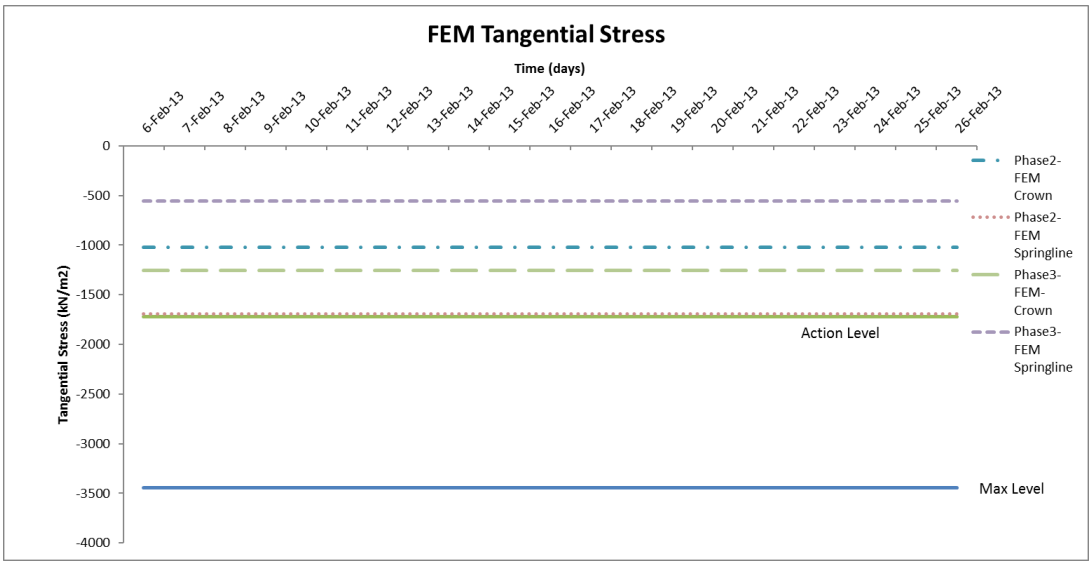

Figure 6.7: FEM Thrust Obtained with Stiffer Ground

Chapter 7. Conclusions

From the Waller Creek Tunnel Finite Element Model performance, some conclusions can be expressed.

- The predictions of liner stresses from FEM are greater than what was measured in the field, particularly for the thrust in the liner.
- While assuming that the ground is 20 times stiffer produces predictions closer to the measurements, the predictions are still greater, particularly for the thrust.
- One possible explanation for the discrepancy between predications and measurements is that the stress cells did not have intimate contact with the liner.
- The Geotechnical Baseline Report does not necessarily provide information needed to predict actual performance.
- The simplified assumption of horizontal layers might introduce some bias to the results of the FEM model. A more accurate of the ground layers would potentially be beneficial.
- More and more accurate information about the tunnel construction sequence would be helpful to refine the construction sequence in the FEM.

References

Curran, J. H., Hammah, R. E., and Yacoub, T. (2003). "A two-dimensional approach for designing tunnel support in weak rock." Proceedings of the 56th Canadian Geotechnical Conference, Winnepeg, Manitoba, Canada, 1–6.

Dao, V.-h. (2009). "Tunnel design considering stress release effect." Water Science and Engineering, 2(3), 87–95.

Einstein, H. (1989). "Suggested methods for laboratory testing of argillaceous swelling rocks." Intl J of Rock Mech & Mining Sci & Geomechanics Abs, 26(5).

Einstein, H. (1994a). "Comments and recommendations on design and analysis procedures for structures in argillaceous swelling rock." International Journal of Rock Mechanics and Mining Sciences and Geomechanics Abstracts, Vol. 31, Oxford; New York: Pergamon Press, 1974-c1996., 535–546.

Einstein, H. (1994b). "Suggested methods for rapid field identification of swelling and slaking rocks." International Journal of Rock Mechanics and Mining Sciences and Geomechanics Abstracts, Vol. 31, Oxford; New York: Pergamon Press, 1974-c1996., 547–550.

Einstein, H. (1996). "Tunnelling in difficult groundswelling behaviour and identification of swelling rocks." Rock mechanics and rock engineering, 29(3), 113–124.

Einstein, H. H., Bischoff, N., et al. (1975). "Design of tunnels in swelling rock." The 16th US Symposium on Rock Mechanics (USRMS), American Rock Mechanics Association.

Fugro. Report No. 4-10013678. Waller Creek Tunnel, Austin, Texas. From: https://www.fugro.com//

Geokon (1993). Pressure Cells: NATM Style Shotcrete Stress (VW) Model 4850. Instruction Manual, Model 4850 NATM Style, VW Concrete Stress Cells. USA. From: http://www.geokon.com//.

Helwa, A. M. (2016). "Predicting the behavior of a drilled shaft wall retaining highly expansive soil." Ph.D. thesis, Ph.D. thesis.

Hoek, E. (2000). Practical rock engineering. Rocscience.

Hoek, E. and Brown, E. T. (1980). Underground excavations in rock. Number Monograph.

Hoek, E., Kaiser, P. K., and Bawden, W. F. (1995). "Support of underground excavations in hard rock.

Hsu, S.-C. and Nelson, P. P. (2002). "Characterization of eagle ford shale." Engineering Geology, 67(1), 169–183.

Jenny and KBR (2010). "Geotechnical Baseline Report – Waller Creek Tunnel Project – Main Tunnel." Submitted to City of Austin, Prepared by Jenny Engineering Corporation, New Jersey and KBR Technical Services, Inc.

Karakus, M. (2007). "Appraising the methods accounting for 3d tunnelling effects in 2d plane strain fe analysis." Tunnelling and Underground Space Technology, 22(1), 47–56.

Karakus, M. and Fowell, R. (2006). "2-d and 3-d finite element analyses for the settlement due to soft ground tunnelling." Tunnelling and Underground Space Technology, 21(3), 392–392.

Kolymbas, D. (2005). Tunnelling and tunnel mechanics: A rational approach to tunnelling. Springer Science & Business Media.

Lachel (2012). "Waller Creek Tunnel Project - Small Diameter Tunnel Initial Support Calculations." Submitted to S.J. Louis Construction, Inc., Prepared by Lachel & Associates, Inc.

MAHTAB, A. and Grasso, P. (1992). Geomechanics principles in the design of tunnels and caverns in rock. Elsevier.

Negro, A. and de Queiroz, B. (2000). "Predication and performance: A review of numerical analyses for tunnels." Geotechnical Aspects of Underground Construction in Soft Ground, Balkema, Rotterdam.

Panet, M. (1995). Le calcul des tunnels par la méthode convergence-confinement. Presses ENPC.

Potts, D. M., Zdravkovic, L., and Zdravkovi´c, L. (2001). Finite element analysis in geotechnical engineering: application, Vol. 2. Thomas Telford.

Principle, O. (2011). NATM Style Shotcrete Stress Cell. Signal, 4850, 1.

Reis, B. K. and Espey, Jr, W. H. (2008). "Waller creek tunnel project, Austin, Texas." World Environmental and Water Resources Congress 2008: Ahupua'A, 1–8.

Ruiz Esparza, G., Murrieta Cummings, R and Poon Hung, C. (2016). Manual de Diseno y Constrcuccion de Tuneles de Carretera 2016. Secretaria de Comunicaciones y Transportes.

Schanz, T., Vermeer, P., and Bonnier, P. (1999). "The hardening soil model: formulation and verification." Beyond 2000 in computational geotechnics, 281–296.

Tjie-Liong, G. (2014). "Common mistakes on the application of plaxis 2d in analyzing excavation problems." International Journal of Applied Engineering Research, 9(21), 8291–8311.

Vardanega, P. and Bolton, M. (2014). "Stiffness of clays and silts: Modeling considerations." Journal of Geotechnical and Geoenvironmental Engineering, 140(6), 06014004.

Vermeer, P. A. (1993). PLAXIS 2D reference manual version 5. *Balkema, Rotterdam/Brookfield*, *70*.

Version, P. (8). Material Models Manual. Delft University of Technology & PLAXIS bv, The Netherlands.

Vita

Alejandro E. Ortiz Pizzoglio was born in San Juan, Argentina on December 26, 1983 to Francisco Walter Ortiz and Rita Lucia Pizzoglio. After graduating as Civil Engineer from Universidad Nacional de San Juan and working for almost five years in tunnel projects in Argentina and Brazil, he was awarded with the Fulbright – Gobierno de San Juan scholarship. In 2015, he become a graduate student at The University of Texas at Austin, where he graduated as Masters of Science in Engineering under Dr. Gilbert supervision in August, 2017.

aleop_sj@hotmail.com

This thesis was typed by the author.